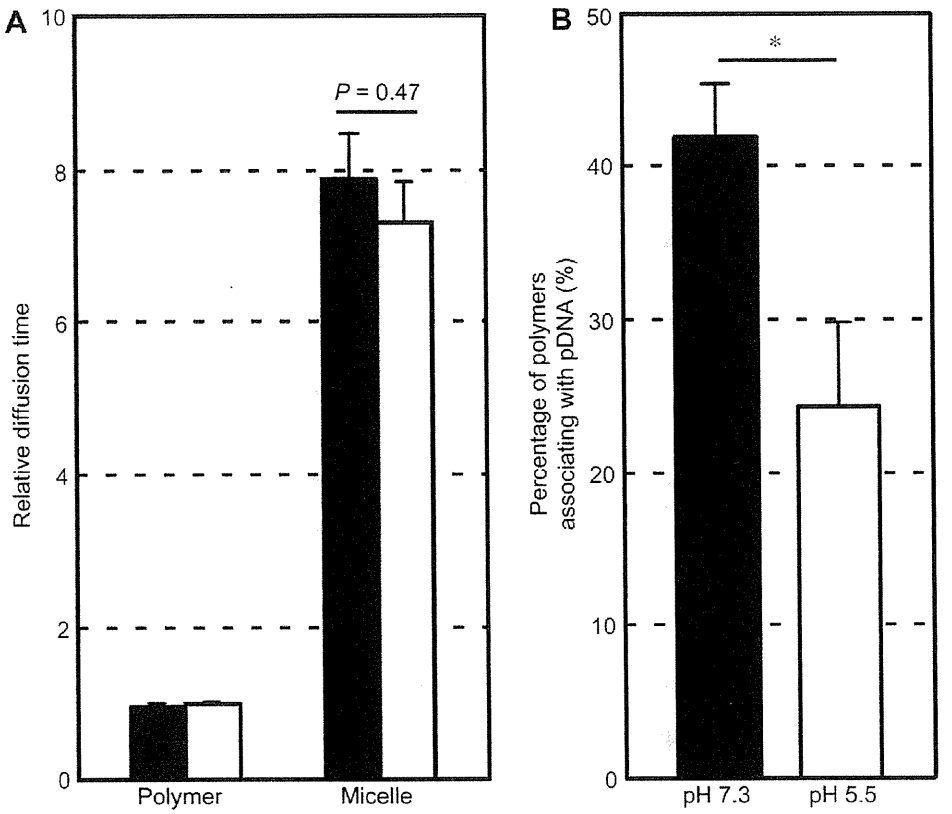

Fig. 10. (A) Relative diffusion time of PEG-PAsp(DET-Alexa680)-Chole block copolymers and their polyplex micelles in the Hepes buffer (pH 7.3). Closed bars: 18.7 μg/mL of block copolymers in the solution. Open bars: 2.08 μg/mL of block copolymers in the solution. (B) Percentage of PEG-PAsp(DET-Alexa680)-Chole block copolymers associating with pDNA in the micelle solutions at different pH. Closed bars: Hepes buffer (pH 7.3). Open bars: MES buffer (pH 5.5). Polyplex micelles were prepared at N/P = 8. Error bars in the graph represent SEM, $n = 7$. $^{*}P < 0.01$.

corroborates well with the result that PEG-PAsp(DET)-Chole micelles achieved high gene transfer under the diluted conditions (Fig. 7B). The amount of polymer associated with pDNA in PEG-PAsp(DET)-Chole micelles (N/P = 8) at pH 7.3 estimated by FCS (42% in Fig. 10B) was in accordance with that calculated from ultracentrifugation analysis (45% in Fig. 4), where 340 of total 756 block copolymers per pDNA were associated with a pDNA. Furthermore, the percentage of polymers associating with pDNA significantly decreased upon lowering the pH from 7.3 to 5.5 (Fig. 10B). Note that ethanediamine units in the side chain of PAsp (DET) adopt a mono-protonated form at pH 7.4 and then become di-protonated at pH 5.5 [11,12]. Thus, this change in the charge state of PAsp(DET) might lead to electrostatic repulsion among block copolymers in the polyplex micelle, thereby releasing a considerable amount of polymers associating with pDNA at pH corresponding to endosomal compartments.

3.12. Stability of polyplex micelles in the blood stream

In order to evaluate the stability of polyplex micelles in the blood, the concentration of Cy5-pDNA in the plasma was measured at various times after intravenous injection of polyplex micelles (N/P = 8) containing Cy5-pDNA via the tail vein of mice (Fig. 11). Almost all the fluorescence from Cy5-pDNA incorporated into PEG-PAsp(DET) micelles disappeared from the blood 30 min after injection. On the other hand, PEG-PAsp(DET)-Chole micelles retained more than 15% and 2% of the injected dose of pDNA in the blood at 30 min and at 60 min after

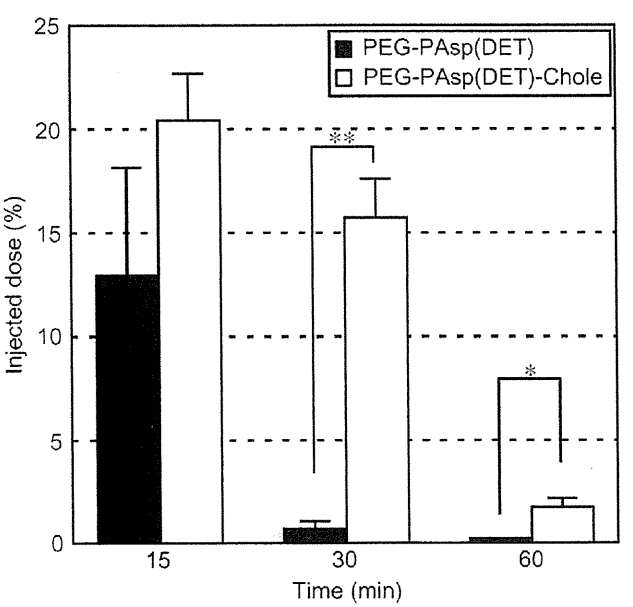

Fig. 11. Cy5-labeled pDNA concentration in the blood after intravenous injection of PEG-PAsp(DET) (closed bars) and PEG-PAsp(DET)-Chole (open bars) polyplex micelles (N/P = 8, 20 μg pDNA/mouse). Error bars in the graph represent SEM, $n = 4$. $^{*}P < 0.05$ and $^{**}P < 0.01$.

injection, respectively. PEG-PAsp(DET)-Chole micelles could hold pDNA more stably in the blood compared to PEG-PAsp(DET) micelles, probably due to their higher stability in proteinous medium (Fig. 5).

3.13. Anti-tumor activity

Polyplex micelles containing sFlt-1 pDNA were injected intravenously into mice-bearing pancreatic adenocarcinoma BxPC3, followed by evaluation of tumor volume (Fig. 12). sFlt-1, which is a soluble form of VEGF receptor-1, is a well-known anti-angiogenic protein [21,22]. We recently reported that systemic injection of polyplex micelles containing sFlt-1 pDNA into mice significantly decreased subcutaneously inoculated BxPC3 growth [16,23], and therefore, this subcutaneous BxPC3 model is appropriate to evaluate the performance of systemic gene delivery vectors. PEG-PAsp (DET) (N/P = 10 and 20) and PEG-PAsp(DET)-Chole (N/P = 15) micelles were administrated every four days for three total doses, i.e. on days 0, 4, and 8. Only the PEG-PAsp(DET)-Chole micelle significantly suppressed tumor growth compared to Hepes buffer (control) ($P < 0.05$).

4. Discussion

PEG-PAsp(DET) micelles are promising gene delivery vectors due to their high transfection ability with low cytotoxicity, however, they must be prepared at high N/P ratio to achieve high transfection efficiency [11,13–15,24]. In general, gene vectors internalized into the cells must escape from the endosome prior to enzymatic degradation in lysosome vesicles for efficient transfection. PAsp(DET) polycations enabled effective escape from the endosome into cytoplasm due to their pH-selective membrane destabilization [12], and thus, a certain amount of PAsp(DET) should be contained within the same endosomal compartment with pDNA to facilitate release. PEG-PAsp(DET) micelles are needed to be prepared at N/P > 20 for effective *in vitro* transfection [11]. In this regard, we showed that almost all the PEG-PAsp(DET) polymers added at N/P ≥ 4, where they may form stoichiometric charged polyplex micelles with pDNA, existed as free polymers by ultracentrifugation analysis (Fig. 1A). Therefore, a large fraction of PEG-PAsp(DET) polymers present in micelle solutions prepared at high N/P ratios are not associated with pDNA in the culture medium but still assist in the endosomal escape of polyplex micelles. Indeed, the transfection efficiency of pDNA micelles prepared with PEG-PAsp(DET) increased with simultaneous addition of free polymer with micelle solution prepared at N/P = 4 to the cell culture medium (open circles in Fig. 1B), whereas similar transfection efficiency (closed circles in Fig. 1B) was observed with PEG-PAsp (DET) micelle solutions prepared at higher N/P ratios (which corresponded to the same amount of free polymer added to culture medium in the experiments with micelle solutions prepared at a constant N/P value of 4). This result indicates that the amount of free polymer in the culture medium is important for improved transfection efficiency, which is consistent with the above-mentioned hypothesis.

In this study, a hydrophobic cholesterol moiety was introduced into the ω-terminus of the PAsp(DET) segment of PEG-PAsp(DET) block copolymer for the purpose of achieving sufficient gene transfer at low N/P ratio and under dilute conditions, thus further developing PEG-PAsp(DET) micelles towards *in vivo* systemic vectors (Scheme 1). PEG-PAsp(DET)-Chole was designed to increase the association number of block copolymers with polyplex micelles by exploiting the hydrophobic nature of cholesterol, which possesses high self-associating ability, to form polyplex micelles over the stoichiometric charge ratio. Indeed, quantification of free polymer in micelle solutions by ultracentrifugation revealed that the number of PEG-PAsp(DET) associating with a pDNA did not change at N/P ≥ 4 ($N^+/P \geq 2$) and that polymer added over N/P = 4 existed as free polymers unassociated with pDNA. On the other hand, PEG-PAsp(DET)-Chole micelles prepared at N/P ≥ 2 ($N^+/P \geq 1$) showed an increase in the number of polymers associated with pDNA with increased N/P ratio (Fig. 4A). Furthermore, the introduction of cholesterol contributed not only to the enhancement of associating ability of polymers to pDNA, but also increased the stability of polyplex micelles. PEG-PAsp(DET)-Chole micelles maintained their structure for 12 h in the presence of BSA with no change in their initial size and PDI (Fig. 5). Note that a stability of a gene delivery vector against serum proteins is an important factor for *in vitro* transfection in the presence of serum and also for *in vivo* transfection via systemic administration and exposure to complex biological milieu in blood. Uptake of pDNA incorporating micelles in culture cells was drastically increased by the introduction of cholesterol (Fig. 8A), likely due to the increased stability of polyplex micelles in the culture medium containing serum. With respect to block copolymer uptake (in experiments performed with micelle solutions prepared with fluorescent-labeled block copolymer), PEG-PAsp(DET)-Chole was internalized into Huh-7 cells significantly more than PEG-PAsp(DET), implying that their uptake is enhanced when associated with polyplex micelles. CLSM observation of the intracellular distribution of polyplex micelles in culture cells revealed that PEG-PAsp(DET)-Chole micelles could more effectively escape from the late endosome/lysosome

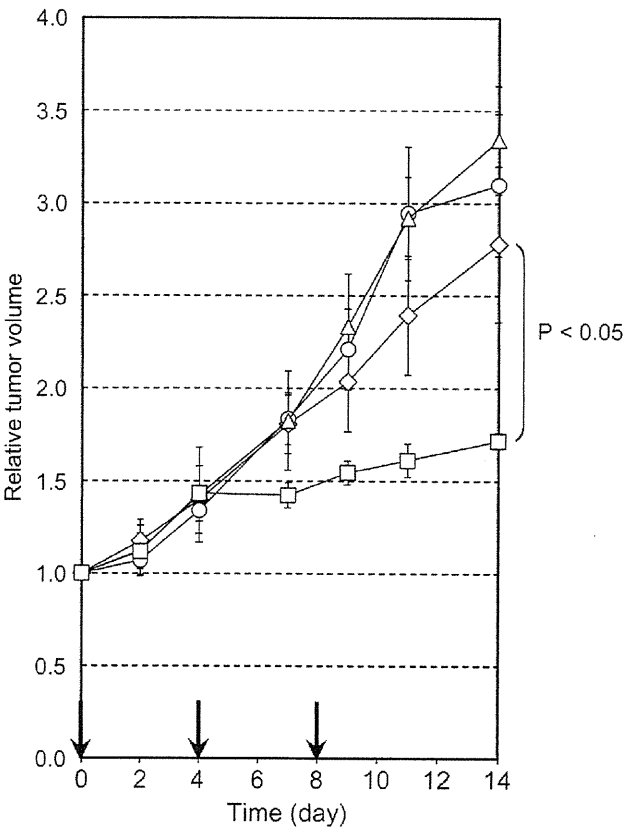

Fig. 12. Anti-tumor activity after intravenous injection of Hepes (diamonds), PEG-PAsp (DET) polyplex micelles at N/P = 10 (circles), at N/P = 20 (triangles), and PEG-PAsp (DET)-Chole polyplex micelles at N/P = 15 (squares). Error bars in the graph represent SEM, $n = 4$.

compartments compared to PEG-PAsp(DET) micelles prepared at the same N/P ratio (Fig. 9). In order for polyplex micelles based on the PEG-PAsp(DET) to be effective gene delivery vectors, block copolymer should be released from polyplex micelles in the endosome and the directly associate with the endosomal membrane to disrupt the vesicle structure and facilitate escape of polyplex micelles into the cytoplasm and allow pDNA to further transport into the nucleus. The relative number of PEG-PAsp(DET)-Chole polymers associating with pDNA estimated by FCS measurement was significantly reduced with decreasing pH, from 42% (pH 7.3) to 24% (pH 5.5) (Fig. 10B). These results suggest that formation of PEG-PAsp(DET)-Chole micelles over stoichiometric charge ratio facilitated effective detachment of block copolymers from polyplex micelles in the acidic endosome by electrostatic repulsion among block copolymers, resulting in efficient endosomal escape based on destabilization of the endosomal membrane. Transfection experiments performed *in vitro* revealed that PEG-PAsp(DET)-Chole micelles achieved high transfection efficiency at lower N/P ratios compared to PEG-PAsp(DET) micelles (Fig. 6A). This enhanced transfection ability is likely due to a synergistic effect between effective uptake of pDNA by increased micelle stability, the ability to form micelles with high polymer association above the stoichiometric N/P value, and efficient endosomal escape by polymers released from the micellar structure upon acidification without increased cytotoxicity, even at high N/P ratios (Fig. 6B).

Gene delivery vectors administered systemically are diluted instantly upon injection, and cannot always reach target sites in high concentration. Therefore, systemic gene vectors must transfect efficiently even under dilute conditions. In this regard, PEG-PAsp(DET)-Chole micelles were confirmed to overcome this issue (Fig. 7). Furthermore, whereas the *in vitro* transfection efficiency of PEG-PAsp(DET) micelles dropped dramatically with decreasing pDNA concentration contained in the culture medium, a decrease in transfection efficiency of PEG-PAsp(DET)-Chole micelles was well prevented. This result corroborates well with the results of FCS measurement of micelle solutions (Fig. 10A), which revealed that the diffusion time of PEG-PAsp(DET)-Chole micelles was not changed by dilution, suggesting that their association state was no altered. The inherent characteristics of PEG-PAsp(DET)-Chole micelles, i.e., high transfection efficiency both at low N/P ratios and under dilute conditions, should be suitable for their use as systemic gene delivery vectors.

The increased stability of polyplex micelles was also confirmed by evaluation of blood circulation after systemic injection into mice via the tail vein (Fig. 11). Naked pDNA is not stable in blood and is reported to be degraded within 5 min after intravenous injection [25]. Although pDNA loaded PEG-PAsp(DET) micelles retained more than 20% of injected dose after 15 min, almost all the pDNA were cleared from the blood after 30 min (Fig. 11). PEG-PAsp(DET) micelles are known to easily decondense in the presence of serum [20], thus, PEG-PAsp(DET) micelles injected directly into the blood stream are likely to decondense and release pDNA, which is subsequently degraded and removed from circulation. On the other hand, PEG-PAsp(DET)-Chole micelles showed significantly prolonged blood circulation compared to PEG-PAsp(DET) micelles (Fig. 11). PEG-PAsp(DET)-Chole micelles, which were stable in the presence of BSA (Fig. 5), likely resist rapid decondensation, leading to longer circulation time.

Polyplex micelles were further evaluated for anti-tumor activity against a murine solid tumor model after intravenous injection in order to evaluate their performance as systemic gene delivery vectors (Fig. 12). Specifically, mice bearing a subcutaneously xenografted BxPC3 human pancreatic adenocarcinoma tumor and therapeutic pDNA encoding the anti-angiogenic protein sFlt-1 were used. As shown in Fig. 12, PEG-PAsp(DET) micelles showed no significant effect, however, PEG-PAsp(DET)-Chole micelles significantly suppressed tumor growth compared to the Hepes buffer control. Important factors affecting the anti-tumor effect of systemically injected gene delivery vectors are stability in the blood and high transfection efficiency within cells at the target site [16]. PEG-PAsp(DET)-Chole micelles exhibited longer blood circulations (Fig. 11) and also maintained high transfection ability even under dilute conditions (Fig. 7) compared to PEG-PAsp(DET) micelles, which correlated to higher therapeutic effect *in vivo*.

5. Conclusion

PEG-PAsp(DET) micelles achieve high transfection efficiency with low cytotoxicity at high N/P ratios, however, the results of this work showed that block copolymer added over the stoichiometric charge ratio exists as free polymers in the micelles solution. In this study, we further improved the design of PEG-PAsp(DET)-based synthetic gene delivery vectors by incorporating a cholesterol moiety into the terminus of PAsp(DET) segment in the block copolymer. PEG-PAsp(DET)-Chole micelles could be formed over the stoichiometric charge ratio due to self-association of cholesterol, and achieved effective endosomal escape due to the efficient delivery of block copolymers and pDNA into target cells and which increased transfection efficiency at low N/P ratios and under the dilute conditions. Furthermore, cholesterol introduction led to increased stability of polyplex micelles in the blood, which resulted in significant suppression of subcutaneous pancreatic tumor growth by intravenous injection of polyplex micelles loading sFlt-1 pDNA. Conventional polyplexes formed with polyethyleneimine or cationic polypeptides have similar issues regarding the impact of free polycations on transfection efficiency as observed with PEG-PAsp(DET) micelles [26,27]. These polyplexes must be used at high N/P ratio or high concentration of pDNA to achieve effective endosomal escape and high transfection efficiency. Thus, the large amount of free polymer can result in increased cytotoxicity *in vitro* and also adverse side effects *in vivo* after intravenous injection. To circumvent the issue of excess polycations not associating with pDNA, polyplexes utilizing hydrophobic groups such as cholesterol have been reported [28,29] and such systems show promise due to excellent transfection efficiency. Nevertheless, those studies focused primarily on increased stability of polyplexes by introduction of cholesterol, with less attention paid to the association number of polymers with polyplexes. In this study, we showed that PEG-PAsp(DET)-Chole micelles with high polymer association could be formed over the stoichiometric charge ratio by detailed evaluation of micelle solutions using ultracentrifugation analysis. Enhanced stability as well as complex formation over the stoichiometric charge ratio contributed to effective gene transfection both *in vitro* and *in vivo*. These findings are extremely helpful for design of non-viral gene vectors and represent a significant improvement towards the use of synthetic polyplex micelle gene delivery vectors as a practical therapeutic modality.

Acknowledgements

This work was financially supported by the Core Research Program for Evolutional Science and Technology (CREST) from Japan Science and Technology Agency (JST) as well as by Grants-in-Aid for Young Scientists (A) (No. 20689024 to M.O.). We express our appreciation to Prof. Masabumi Shibuya (Tokyo Medical and Dental University) for providing pVL 1393 baculovirus vector pDNA encoding human sFlt-1. We thank Ms. Junko Kawakita and Ms. Satomi Ogura (The University of Tokyo) for technical assistance.

Appendix

Figures with essential color discrimination. Fig. 9 in this article may be difficult to interpret in black and white. The full color images can be found in the on-line version, at doi:10.1016/j.biomaterials.2010.09.022.

References

[1] Mastrobattista E, van der Aa MAEM, Hennink WE, Crommelin DJA. Artificial viruses: a nanotechnological approach to gene delivery. Nat Rev Drug Discov 2006;5:115–21.

[2] Mintzer M, Simanek EE. Nonviral vectors for gene delivery. Chem Rev 2009;109:259–302.

[3] Kakizawa Y, Kataoka K. Block copolymer micelles for delivery of gene and related compounds. Adv Drug Deliv Rev 2002;54:203–22.

[4] Merdan T, Kopecek J, Kissel T. Prospects for cationic polymers in gene and oligonucleotide therapy against cancer. Adv Drug Deliv Rev 2002;54:715–58.

[5] Pack DW, Hoffman AS, Pun S, Stayton PS. Design and development of polymers for gene delivery. Nat Rev Drug Discov 2005;4:581–93.

[6] Kataoka K, Togawa H, Harada A, Yasugi K, Matsumoto T, Katayose S. Spontaneous formation of polyion complex micelles with narrow distribution from antisense oligonucleotide and cationic block copolymer in physiological saline. Macromolecules 1996;29:8556–7.

[7] Katayose S, Kataoka K. Water-soluble polyion complex associates of DNA and poly(ethylene glycol)-poly(L-lysine) block copolymer. Bioconjug Chem 1997;8:702–7.

[8] Kabanov AV, Kabanov VA. Interpolyelectrolyte and block ionomer complexes for gene delivery: physicochemical aspects. Adv Drug Deliv Rev 1998;30:49–60.

[9] Osada K, Christie JR, Kataoka K. Polymeric micelles from poly(ethylene glycol)-poly(amino acid) block copolymer for drug and gene delivery. J R Soc Interface 2009;6:S325–39.

[10] Itaka K, Kataoka K. Recent development of nonviral gene delivery systems with virus-like structures and mechanism. Eur J Pharm Biopharm 2009;71:475–83.

[11] Kanayama N, Fukushima S, Nishiyama N, Itaka K, Jang WD, Miyata K, et al. A PEG-based biocompatible block catiomer with high buffering capacity for the construction of polyplex micelles showing efficient gene transfer toward primary cells. Chem Med Chem 2006;1:439–44.

[12] Miyata K, Oba M, Nakanishi M, Fukushima S, Yamasaki Y, Koyama H, et al. Polyplexes from poly(aspartamide) bearing 1,2-diaminoethane side chains induce pH selective, endosomal membrane destabilization with amplified transfection and negligible cytotoxicity. J Am Chem Soc 2008;130:16287–94.

[13] Akagi D, Oba M, Koyama H, Nishiyama N, Fukushima S, Miyata T, et al. Biocompatible micellar nanovectors achieve efficient gene transfer to vascular lesions without cytotoxicity and thrombus formation. Gene Ther 2007;14:1029–38.

[14] Itaka K, Ohba S, Miyata K, Kawaguchi H, Nakamura K, Takato T, et al. Bone regeneration by regulated in vivo gene transfer using biocompatible polyplex nanomicelles. Mol Ther 2007;15:1655–62.

[15] Harada-Shiba M, Takamisawa I, Miyata K, Ishii T, Nishiyama N, Itaka K, et al. Intratracheal gene transfer of adrenomedullin using polyplex nanomicelles attenuates monocrotaline-induced pulmonary hypertension in rats. Mol Ther 2009;17:1180–6.

[16] Oba M, Vachutinsky Y, Miyata K, Kano MR, Ikeda S, Nishiyama N, et al. Antiangiogenic gene therapy of solid tumor by systemic injection of polyplex micelles loading plasmid DNA encoding soluble Flt-1. Mol Pharmaceutics 2010;7:501–9.

[17] Oba M, Aoyagi K, Miyata K, Matsumoto Y, Itaka K, Nishiyama N, et al. Polyplex micelles with cyclic RGD peptide ligands and disulfide cross-links directing to the enhanced transfection via controlled intracellular trafficking. Mol Pharmaceutics 2008;5:1080–92.

[18] Nakanishi M, Park JS, Jang WD, Oba M, Kataoka K. Study of the quantitative aminolysis reaction of poly(β-benzyl L-aspartate) (PBLA) as a platform polymer for functionality materials. React Funct Polym 2007;67:1361–72.

[19] Takae S, Miyata K, Oba M, Ishii T, Nishiyama N, Itaka K, et al. PEG-detachable polyplex micelles based on disulfide-linked block catiomers as bioresponsive nonviral gene vectors. J Am Chem Soc 2008;130:6001–9.

[20] Miyata K, Fukushima S, Nishiyama N, Yamasaki Y, Kataoka K. PEG-based block catiomers possessing DNA anchoring and endosomal escaping functions to form polyplex micelles with improved stability and high transfection efficacy. J Control Release 2007;122:252–60.

[21] Shibuya M, Yamaguchi S, Yamane A, Ikeda T, Tojo A, Matsushime H, et al. Nucleotide sequence and expression of a novel human receptor-type tyrosine kinase gene (flt) closely related to the fms family. Oncogene 1990;5:519–24.

[22] Kendall RL, Thomas KA. Inhibition of vascular endothelial cell growth factor activity by an endogenously encoded soluble receptor. Proc Natl Acad Sci U S A 1993;90:10705–9.

[23] Vachutinsky Y, Oba M, Miyata K, Hiki S, Kano MR, Nishiyama N, et al. Antiangiogenic gene therapy of experimental pancreatic tumor by sFlt-1 plasmid DNA carried by RGD-modified crosslinked polyplex micelles. J Control Release (in press).

[24] Han M, Bae Y, Nishiyama N, Miyata K, Oba M, Kataoka K. Transfection study of using multicellular tumor spheroids for screening non-viral polymeric gene vectors with low cytotoxicity and high transfection efficiencies. J Control Release 2007;121:38–48.

[25] Harada-Shiba M, Yamauchi K, Harada A, Takamisawa I, Shimokado K, Kataoka K. Polyion complex micelles as vectors in gene therapy-pharmacokinetics and in vivo gene transfer. Gene Ther 2001;9:407–14.

[26] Boeckle S, von Gersdorff K, van der Piepen S, Culmsee C, Wagner E, Ogris M. Purification of polyethylenimine polyplexes highlights the role of free polycations in gene transfer. J Gene Med 2004;6:1102–11.

[27] Fahrmeir J, Gunther M, Tietze N, Wagner E, Ogris M. Electrophoretic purification of tumor-targeted polyethylenimine-based polyplexes reduces toxic side effects in vivo. J Control Release 2007;122:236–45.

[28] Han SO, Mahato RI, Kim SW. Water-soluble lipopolymer for gene delivery. Bioconjug Chem 2001;12:337–45.

[29] Guo XD, Tandiono F, Wiradharma N, Khor D, Tan CG, Khan M, et al. Cationic micelles self-assembled from cholesterol-conjugated oligopeptides as an efficient gene delivery vector. Biomaterials 2008;29:4838–46.

Journal of Controlled Release 145 (2010) 141–148

Contents lists available at ScienceDirect

Journal of Controlled Release

journal homepage: www.elsevier.com/locate/jconrel

GENE DELIVERY

Introduction of stearoyl moieties into a biocompatible cationic polyaspartamide derivative, PAsp(DET), with endosomal escaping function for enhanced siRNA-mediated gene knockdown

Hyun Jin Kim [a], Atsushi Ishii [b], Kanjiro Miyata [c,d], Yan Lee [c,d], Shourong Wu [a], Makoto Oba [e], Nobuhiro Nishiyama [c,d], Kazunori Kataoka [a,c,d,*]

[a] Department of Materials Engineering, Graduate School of Engineering, The University of Tokyo, 7-3-1 Hongo, Bunkyo-ku, Tokyo 113-8656, Japan
[b] NanoCarrier Co., Ltd., 5-4-19 Kashiwanoha, Kashiwa, Chiba 277-0882, Japan
[c] Center for NanoBio Integration, The University of Tokyo, 7-3-1 Hongo, Bunkyo-ku, Tokyo 113-8656, Japan
[d] Center for Disease Biology and Integrative Medicine, Graduate School of Medicine, The University of Tokyo, 7-3-1 Hongo, Bunkyo-ku, Tokyo 113-0033, Japan
[e] Department of Clinical Vascular Regeneration, Graduate School of Medicine, The University of Tokyo, 7-3-1 Hongo, Bunkyo-ku, Tokyo 113-0033, Japan

ARTICLE INFO

Article history:
Received 12 January 2010
Accepted 24 March 2010
Available online 30 March 2010

Keywords:
RNAi
siRNA delivery
Polyplex
Stearoylation
Polyaspartamide

ABSTRACT

Applications of siRNA for cancer therapy have been spotlighted in recent years, but the rational design of efficient siRNA delivery carriers is still controversial, especially because of possible toxicity of the carrier components. Previously, a cationic polyaspartamide derivative, poly{*N*-[*N*-(2-aminoethyl)-2-aminoethyl] aspartamide} (PAsp(DET)), was reported to exert high transfection efficacy for plasmid DNA with negligible cytotoxicity. However, its direct application for siRNA delivery was fairly limited due to the unstable polymer/siRNA complex formation. In this study, to overcome such instability, stearic acid as a hydrophobic moiety was conjugated to the side chain of PAsp(DET) with various substitution degrees. The stearoyl introduction contributed not only to siRNA complex formation with higher association numbers but also to complex stabilization. The obtained stearoyl PAsp(DET)/siRNA complex significantly accomplished more efficient endogenous gene (BCL-2 and VEGF) knockdown *in vitro* against the human pancreatic adenocarcinoma (Panc-1) cells than did the unmodified PAsp(DET) complex and commercially available reagents, probably due to the facilitated cellular internalization. This finding suggests that the hydrophobic PAsp(DET)-mediated siRNA delivery is a promising platform for *in vivo* siRNA delivery.

1. Introduction

RNA interference (RNAi) is a powerful regulatory mechanism of the target mRNA degradation induced by the complementary RNA strand. Because of the selectivity of the targeted mRNA degradation as well as the potential of silencing almost all the endogenous genes, small interfering RNA (siRNA) has been highlighted as an attractive choice for future therapeutics. The advent of siRNA opened a new era of therapy for cancers, autoimmune diseases, and dominant genetic disorders by the selective control of disease-related gene expression [1].

In spite of its promise, the *in vivo* therapeutic application of siRNA needs to overcome several biological hurdles [2]. Naked siRNA is easily degraded by nucleases in the blood-stream and also is cleared by the kidneys within several minutes [3]. The negative charge of the siRNA inhibits its interaction with negatively charged plasma membrane for the internalization into cells. Even though some portions of siRNAs could be internalized into cells, the internalized siRNA would be degraded in lysosome. Hence, a carrier system to protect siRNA from these external circumstances and to allow it to escape the endosome efficiently before the lysosomal degradation is required for effective siRNA therapeutics.

Various siRNA carriers such as lipid-based carriers (lipoplexes) [4] and polycation-based carriers (polyplexes) [5] have been developed to fulfill such requirements, including cellular uptake and endosomal escape of siRNA. For example, polyethylenimine (PEI) has been widely studied for siRNA delivery as well as plasmid DNA delivery due to its powerful endosomal escape ability, based on the proton sponge hypothesis [5,6]. Despite the partial success of such delivery vehicles, toxicity issues derived from the carrier components limit practical applications. Thus, the design of a carrier for efficient siRNA delivery with limited cytotoxicity is of great importance. We previously reported that the cationic polyaspartamide derivative, poly{*N*-[*N*-(2-aminoethyl)-2-aminoethyl]aspartamide} (PAsp(DET)), possessed pH-sensitive endosome destabilizing activity [7]. PAsp(DET) can destabilize the cellular membrane only at the endosomal pH, probably because the mono-protonated form of 1, 2-diaminoethane moiety in the PAsp(DET) side chain at neutral pH is converted to the di-

* Corresponding author. Department of Materials Engineering, Graduate School of Engineering, The University of Tokyo, 7-3-1 Hongo, Bunkyo-ku, Tokyo 113-8656, Japan. Tel.: +81 3 5841 7138; fax: +81 3 5841 7139.
E-mail address: kataoka@bmw.t.u-tokyo.ac.jp (K. Kataoka).

0168-3659/$ – see front matter © 2010 Elsevier B.V. All rights reserved.
doi:10.1016/j.jconrel.2010.03.019

protonated form at the acidic pH condition in the endosome. PAsp (DET)-based polyplexes with plasmid DNA have remarkable transfection efficiency without marked cytotoxicity in various cultured cells, including primary cells [8,9]. Also, our recent studies have revealed the *in vivo* utilities of PAsp(DET) polyplexes through several animal experiments: (i) local transfection into a rabbit's clamped carotid artery with neointima via intra-arterial injection [10] and into mouse lungs via intra-tracheal injection [11], (ii) systemic delivery into subcutaneous pancreatic tumors via intravenous injection into a mouse tail vein [12], and (iii) transfection into a mouse skull via the regulated release from a calcium phosphate cement scaffold [13].

Although PAsp(DET) polyplexes showed significant success in delivering plasmid DNA into cells, their direct application to siRNA delivery was appreciably limited due to the instability of the polymer/siRNA complexes under physiological conditions. One of the reasons for such lower stability of the PAsp(DET)/siRNA complex is explained by the short and rigid structure of siRNA (21 base pairs long) compared to plasmid DNA (over 3000 base pairs long). The condensation of a single plasmid DNA by polycations provides the polyplex with a stable core, whereas such condensation does not occur with much shorter siRNAs [14]. Therefore, an additional association force is needed for stable siRNA complex formation.

As for an additional association force, hydrophobic interaction is a promising candidate for stabilization of siRNA complex based on the polyion complex formation. Indeed, hydrophobic group-modified polycations, such as poly(*N*-methyldiethenеamine sebacate) (PMDS), PEI, and oligo-arginine, were tested for siRNA delivery, resulting in the formation of stable complexes [15–17]. Here, we report the development of hydrophobic polycations with high complex stability as well as low cytotoxicity by using PAsp(DET) as the backbone polycation and stearoyl groups as a hydrophobic moiety. To optimize the interaction between hydrophobic polycations and siRNA, stearoyl PAsp(DET) was synthesized with varying substitution degrees and characterized from the view-point of siRNA complex stability and RNAi activity in cultured cells. Furthermore, the efficient RNAi obtained from stearoyl PAsp(DET)/siRNA complexes motivated us to investigate the transfection mechanism, which revealed cellular internalization and intracellular trafficking to be key steps.

2. Materials and methods

2.1. Materials

β-Benzyl-L-aspartate *N*-carboxy-anhydride (BLA-NCA) was synthesized according to Fuchs's method [18]. *N,N*-Dimethylformamide (DMF), dichloromethane (DCM), *n*-butylamine, diethylenetriamine (DET), methanol (MeOH), *N*-hydroxysuccinimide (NHS), and *N*-methyl-2-pyrrolidone (NMP) were purchased from Wako Pure Chemical Industries, Ltd. (Osaka, Japan). Poly(L-lysine) hydrobromide (M_w = 15,000–30,000), Dulbecco's modified Eagle's medium (DMEM), DMEM without L-glutamine and phenol red, diisopropylethylamine (DIPEA), stearic acid, and 0.4% trypan blue solution were purchased from Sigma-Aldrich Co. (St. Louis, Mo). 1-Ethyl-3-(3-dimethylaminopropyl)-carbodiimide, hydrochloride (EDC) was purchased from Dojindo (Kumamoto, Japan). DMF, *n*-butylamine, DET, and DIPEA were distilled with the conventional methods before use. The human pancreatic adenocarcinoma cell line, Panc-1, was obtained from the American Type Culture Collection (Manassas, VA). The luciferase-expressing mouse melanoma cell line, B16F10-Luc was purchased from Caliper LifeScience (Hopkinton, MA). Fetal bovine serum (FBS) was purchased from Dainippon Sumitomo Parma Co., Ltd. (Osaka, Japan). Lipofectamine 2000 and ExGen500 were purchased from Invitrogen (Carlsbad, CA) and Fermentas (Ontario, Canada), respectively. Firefly luciferase siRNA (sense: 5′-CUU ACG CUG AGU ACU UCG AdTdT-3′; antisense: 5′-UCG AAG UAC UCA GCG UAA GdTdT-3′), Cy5-labeled firefly luciferase siRNA, Cy3-labeled firefly luciferase siRNA, Enhanced Green Fluorescence Protein (EGFP) siRNA (sense: 5′-GCA GCA CGA CUU CUU CAA GdTdT-3′; antisense: 5′-CUU GAA GAA GUC GUG CUG CdTdT-3′), BCL-2 (human BCL-2, M13994) siRNA (sense: 5′-CAG GAC CUC GCC GCU GCA GAC-3′; antisense: 3′-CGG UCC UGG AGC GGC GAC GUC UG-5′ [19]), and VEGF (human VEGF, NM_001025366) siRNA (sense: 5′-GGA GUA CCC UGA UGA GAU CdTdT-3′; antisense: 5′-GAU CUC AUC AGG GUA CUC CdTdT-3′) were synthesized by Hokkaido System Science Co., Ltd. (Hokkaido, Japan).

2.2. Synthesis

Synthesis methods are available in Supplementary data.

2.3. Preparation and characterization of siRNA complex with stearoyl PAsp(DET)

Polycations were dissolved in 10 mM HEPES buffer (pH 7.3) or 50% ethanol solution (ethanol/10 mM HEPES buffer, 1:1 v/v) and then mixed with 20 μM siRNA solution (10 mM HEPES buffer, pH 7.3) to form siRNA complexes (5 μM of siRNA) at the desired N/P ratio. Complex size and zeta potential were determined using a Zetasizer (Malvern Instruments, Worcestershire, U.K.) with a He–Ne Laser (λ = 633 nm) for the incident beam at a detection angle of 173° and a temperature of 25 °C. The size measurement was performed in a low-volume quartz cuvette (ZEN2112, Malvern Instruments, volume 12 μL). The data obtained from the rate of decay in the photon correlation function were analyzed by the cumulant method and the corresponding hydrodynamic diameter of the complexes was then calculated by the Stokes–Einstein equation. For zeta potential measurements, each complex solution was placed in a folded capillary cell (Malvern Instruments). Zeta potential was calculated from the measured electrophoretic mobility using the Smoluchowski equation.

2.4. Diffusion coefficient measurement by fluorescence correlation spectroscopy (FCS)

FCS experiments were performed using a Confocor3 module (Carl Zeiss, Jena, Germany) equipped with a Zeiss C-Apochromat 40× water objective. A HeNe laser (543 nm) was used for Cy3-labeled siRNA excitation and emission was filtered through a 560–615 nm band pass filter. Samples were placed into 8-well Lab-Tek chambered borosilicate cover-glass (Nalge Nunc International, Rochester, NY) and measured at room temperature. siRNA stock was prepared to contain 1% Cy3-labeled siRNA concentration, and each analysis of naked Cy3-siRNA, PAsp(DET)/Cy3-siRNA, stearoyl PAsp(DET)/Cy3-siRNA complexes (5 μM siRNA, N/P 5.0), and Rhodamine 6G as a reference in 10 mM HEPES buffer (pH 7.3) consisted of 10 measurements with a sampling time of 20 s. The measured autocorrelation curves were fitted with the Zeiss Confocor3 software package to obtain the diffusion coefficient, *D*.

Stability of siRNA complexes in the cell culture condition was evaluated in DMEM without L-glutamine and phenol red containing 10% FBS (DMEM/FBS). siRNA stock was prepared to contain 2% Cy3-labeled siRNA concentration, and each sample of naked Cy3-siRNA, PAsp(DET)/Cy3-siRNA, stearoyl PAsp(DET)/Cy3-siRNA complexes (5 μM siRNA, N/P 5.0) was diluted 10 times with DMEM/FBS and incubated at designated period before measurements.

2.5. Endogenous luciferase gene knockdown in B16F10-Luc

Luciferase-expressing B16F10 cells were seeded into a 96-well plate at a density of 5000 cells/well in DMEM containing 10% FBS. Firefly luciferase and EGFP siRNA complexes were transfected at 100 nM siRNA. After 48 h incubation, the media was exchanged and the cells were incubated for another 24 h. Luciferase gene knockdown was measured using the Luciferase Assay System (Promega) in

a luminescence microplate reader (Mithras LB 940, Berthold technologies, Bad Wildbad, Germany).

2.6. BCL-2 endogenous gene knockdown by real-time PCR

Panc-1 cells were seeded into a 6-well plate at a density of 100,000 cells/well in DMEM containing 10% FBS. BCL-2 siRNA complexes were transfected at 100 nM siRNA. After 48-hour incubation, total RNA was collected with an RNeasy Mini kit (Qiagen). Reverse transcription PCR was carried out using a TAKARA PrimeScript RT reagent kit and real-time PCR was measured using a QuantiTect SYBR Green PCR kit (Qiagen) with an ABI 7500 Fast Real-Time PCR System (Applied Biosystems, Foster City, CA). GAPDH was used as an internal control for the real-time PCR amplification. The mRNAs of BCL-2 and GAPDH were amplified with TAKARA BCL-2 and GAPDH primers (Primer Set ID HA032557 and HA067812, respectively). All procedures followed the manufacturer's protocol.

2.7. VEGF endogenous gene knockdown in real-time PCR

Endogenous VEGF gene suppression in Panc-1 cells was evaluated using the same procedure as BCL-2 gene knockdown with actin used as the internal control. VEGF was amplified using 5′-AGT GGT CCC AGG CTG CAC-3′ as the forward primer and 5′-TCC ATG AAC TTC ACC ACT TCG T-3′ as the reverse primer. Actin was amplified using 5′-CCT GGC ACC CAG CAC AAT G-3′ as the forward primer and 5′-CGC CGA TCC ACA CGG AGT A-3′ as the reverse primer. All experiments were performed in triplicate and data was normalized to actin expression.

2.8. Flow cytometer measurement

B16F10 cells were seeded into a 6-well plate at a density of 100,000 cells/well in DMEM containing 10% FBS. Cy5-labeled siRNA complexes were prepared for each polymer (N/P 5.0) and transfected at 100 nM siRNA. After 3-hour incubation, the media was removed and the cells were washed with 0.5 mL of PBS. The cells were treated with a trypsin-EDTA solution for 2 min and suspended in PBS. The intracellular uptake of the siRNA complexes was measured using a BD™ LSR II flow cytometer (BD Biosciences).

2.9. Confocal laser scanning microscope (CLSM)

Panc-1 cells were seeded into a 35-mm glass-based dish (Iwaki, Tokyo, Japan) at a density of 50,000 cells/well in DMEM containing 10% FBS. The Cy3-labeled siRNA complex of each polymer (N/P 5.0) was transfected at 100 nM siRNA. After the designated incubation period, each dish was observed using a CLSM (ZEISS LSM 510, Carl Zeiss, Oberlochen, Germarny) equipped with a C-Apochromat 63× objective (Carl Zeiss). Late-endosomes/lysosomes were stained by LysoTracker Green (Molecular Probes, Eugene, OR) for 1.5 h and nuclei were stained with Hoechst 33342 (Dojindo, Japan) for 10 min before each observation. 0.4% trypan blue solution was added to media just before observation to quench extracellular-bound Cy3-labeled siRNA [20]. The excitation wavelengths used were 488 nm (Ar laser) for LysoTracker, 543 nm (He–Ne laser) for Cy3-labeled siRNA, and 710 nm (MaiTai laser; two photon excitation; Spectra Physics, Mountain View, CA) for Hoechst 33342.

Statistical colocalization was calculated from Spearman's rank correlation coefficient [21];

$$\rho_S = 1 - 6\sum \frac{d_i^2}{n(n^2-1)},$$

where a set of n pairs of numbers (x_i, y_i) means the values recorded from the red and green channels of a image, and d_i is the difference between the rank position in the (x_i, y_i) data pair. Because Spearman's rank correlation coefficient can remove the effects of brightness difference between two images, it is suitable for excluding the parameter for the amount of intracellular uptake of Cy3-labeled siRNA.

2.10. Cell viability assay

Cell viability was determined using a Cell Counting Kit-8 (Dojindo, Japan). Panc-1 cells were seeded into a 24-well plate at a density of 20,000 cells/well in DMEM containing 10% FBS. After overnight incubation, siRNA complexes were introduced and cells were then incubated for another 48 h. The growth medium was exchanged with fresh media (500 μl) containing the manufacturer's reagent (50 μl) and the cells were then incubated for 1.5 h. The absorbance of the media was measured at 450 nm using a microplate reader (Biorad).

3. Results and discussion

3.1. Synthesis of stearoyl PAsp(DET) and stearoyl PLL

Stearoyl PAsp(DET) was synthesized by amide bond formation between N-succinimidyl octadecanoate and the primary amine of PAsp (DET) (Scheme 1). The feed ratio was defined as the relative molar ratio of *N*-succinimidyl octadecanoate to primary amines of PAsp(DET) in the reaction mixture. The resulting introduction rate of the stearoyl amide was calculated from the peak intensity ratio between the methyl protons of stearoyl moieties (CH_3–, $\delta = 1.19$ ppm) and β-protons of aspartate groups in PAsp(DET) (–CH_2–, $\delta = 3.16$ ppm) in the ^{1}H NMR spectra (data not shown). Three different substituted stearoyl PAsp (DET)s (12%, 19%, and 32%) were prepared by varying the feed ratio.

As a control polycation without endosomal disrupting ability, 23% stearoyl PLL was synthesized in the same fashion by amide bond formation between *N*-succinimidyl octadecanoate and primary amines of PLL. The feed ratio was calculated from the relative molar ratio of *N*-succinimidyl octadecanoate to primary amines of PLL. The resulting stearoyl substitution rate was obtained from the peak intensity ratio between the methyl protons of stearoyl moieties and ε-protons of the lysine groups (–CH_2–, $\delta = 3.04$–3.17 ppm) in the ^{1}H NMR spectra (data not shown). A series of the hydrophobic polycations were abbreviated as PAsp(DET)-ST12, PAsp(DET)-ST19, PAsp(DET)-ST32 for 12%, 19%, 32% stearoyl PAsp(DET), respectively, and as PLL-ST23 for 23% stearoyl PLL.

3.2. Formation of siRNA complex with stearoyl PAsp(DET)

Formation of siRNA complexes with stearoyl PAsp(DET) was evaluated by gel electrophoresis at various N/P ratios. The N/P ratio is defined as the molar ratio of the total amines in PAsp(DET) (N) to the phosphates in siRNA (P). Note that stearoyl introduction concurrently reduces the number of primary amines (N) of PAsp(DET) with increasing degree of substitution. Thus, the total amines in stearoyl PAsp(DET) do not include the primary amines of PAsp(DET) which were converted to amide bonds after stearoyl introduction. Because the 1, 2-diaminoethane side chain in PAsp(DET) takes a monoprotonated form at pH 7.3 [7], The free siRNA band disappears above the stoichiometric N/P ratio of complete siRNA formation (N/P = 2) (Fig. S1). However, smear bands were detected at higher molecular weight positions at N/P = 2.5–4.5. Thus N/P ≥ 5 was selected for further experiments because all of the PAsp(DET) and stearoyl PAsp(DET) derivatives showed the disappearance of the free siRNA and smear band, indicating that all the siRNA molecules were associated with polycations.

The size and zeta potential of siRNA complexes with stearoyl PAsp (DET) in 10 mM HEPES buffer (pH 7.3) were determined by dynamic light scattering (DLS) and electrophoretic mobility measurements, respectively, and the results are summarized in Table 1. Stearoyl PAsp(DET) complexes (N/P 5–N/P 10) ranged in size from 120 nm to

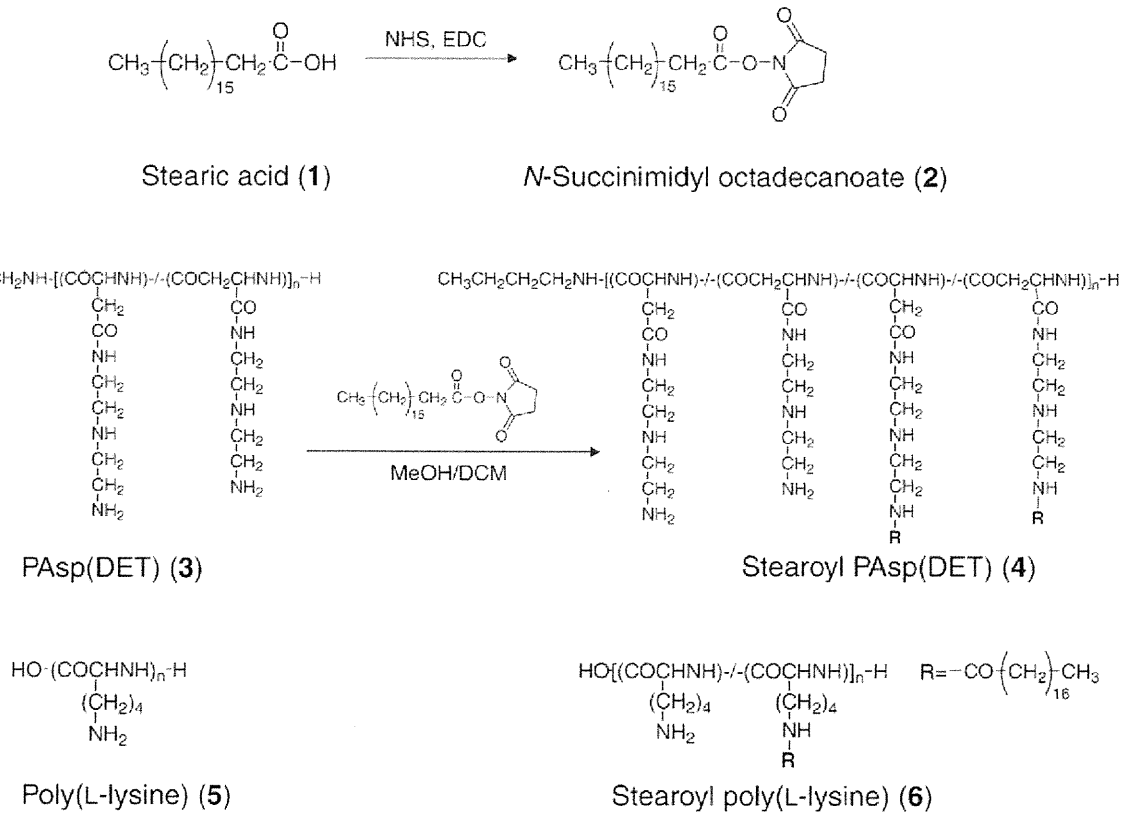

Scheme 1. Synthetic routes of *N*-succinimidyl octadecanoate (2), stearoyl PAsp(DET) (4), and stearoyl poly(L-lysine) (6).

200 nm with a polydispersity index (PDI) of less than 0.2. Zeta potentials of the siRNA complexes showed relatively constant values (+30 mV to −40 mV) irrespective of the stearoylation degree. On the other hand, the siRNA complex formed with unmodified PAsp (DET) exhibited appreciably low scattered light intensity close to the background of the solvent. In this regard, complex formation was further evaluated by FCS with Cy3-labeled siRNA, which allows determination of the diffusion coefficient of a complex in a very small volume (~femto L) [22,23]. All the stearoyl PAsp(DET) complexes had a one order of magnitude lower diffusion coefficient than naked siRNA and unmodified PAsp(DET) complex (Table 2). Considering that the diffusion coefficient is reversely correlated to the hydrodynamic diameter of the complexes, with the assumption that siRNA complexes are spherical, the obtained result confirmed that stearoyl introduction would contribute to the formation of larger complexes with higher association numbers, compared to the unmodified PAsp (DET). It is worth noting that the diffusion coefficients of the PAsp (DET)-ST12, ST19, and ST32 complexes measured by FCS are roughly correlated to those measured by DLS (3.27 ± 0.13, 2.79 ± 0.32, and 2.59 ± 0.26 μm²/s).

The stability of stearoyl PAsp(DET)/siRNA complex was investigated in cell culture conditions. The diffusion coefficient was monitored over time by FCS to estimate the dissociation tendency of siRNA complexes in DMEM containing 10% FBS (Fig. 1). The diffusion coefficient of unmodified PAsp(DET)/siRNA complex was increased to that of naked siRNA with increased incubation period, indicating that the unmodified PAsp(DET)/siRNA complex was completely dissociated in a 3-hour incubation period. In contrast, stearoyl PAsp(DET)/siRNA complexes maintained their initial diffusion coefficient for a 3-hour incubation period. This result indicates the higher stability of stearoyl PAsp(DET) complexes than the unmodified PAsp(DET) complex in the serum-containing media. These results reveal that the stearoyl PAsp(DET) complex tolerates the cell culture condition better than does the unmodified PAsp(DET) complex, allowing for improved cellular internalization.

3.3. Gene expression inhibition by stearoyl PAsp(DET)/siRNA complexes

To determine the optimal stearoylation degree for efficient gene knockdown, the luciferase gene knockdown ability of stearoyl PAsp (DET)/siRNA complexes was measured in luciferase-expressing B16F10

Table 1
Size and zeta potential of stearoyl PAsp(DET)/siRNA complexes.

Stearoyl introduction rate	N/P	Size (nm) ± S.D.	Zeta potential (mV) ± S.D.
12%	5	150 ± 6	39.7 ± 8.0
	7.5	136 ± 2	39.0 ± 8.5
	10	122 ± 5	37.4 ± 9.7
19%	5	196 ± 1	29.5 ± 6.1
	7.5	134 ± 4	36.8 ± 5.2
	10	129 ± 1	36.0 ± 5.3
	15	141 ± 1	38.2 ± 6.6
32%	5	187 ± 24	32.0 ± 5.0
	7.5	177 ± 45	34.5 ± 5.1
	10	192 ± 23	35.5 ± 5.0

Table 2
Diffusion coefficient of stearoyl PAsp(DET)/Cy3-siRNA complexes.

	Diffusion coefficient (μm²/s) ± S.D.
Naked Cy3-siRNA	56.26 ± 0.18
Unmodified PAsp(DET)	33.88 ± 0.14
PAsp(DET)-ST12	2.17 ± 0.03
PAsp(DET)-ST19	1.89 ± 0.03
PAsp(DET)-ST32	1.46 ± 0.02

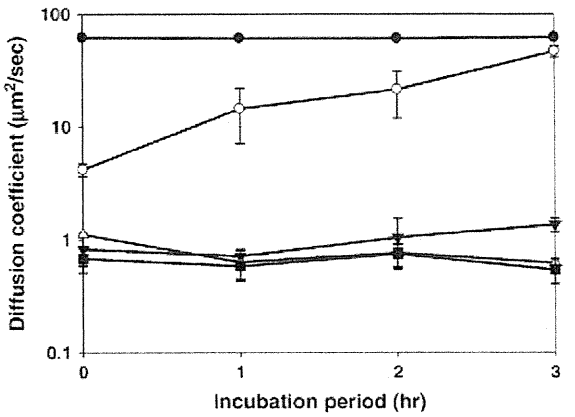

Fig. 1. Time-dependent change in diffusion coefficients of siRNA complexes in the cell culture medium measured by FCS. Curves show naked siRNA (●), unmodified PAsp (DET)/siRNA (○), PAsp(DET)–ST12 (▼), PAsp(DET)–ST19 (△), and PAsp(DET)–ST32 (■)complexes.

cells (Fig. 2). siRNA complexes were prepared with stearoyl PAsp(DET) comprising different stearoyl introduction ratios at various N/P ratios. The luminescence intensity of non-treated cells was set as 1.0, and EGFP siRNA was used as a negative control. Unmodified PAsp(DET) complex showed almost no luciferase gene knockdown at the tested N/Ps. However, stearoyl introduction significantly enhanced the gene suppression efficacy. Especially, the PAsp(DET)–ST19 showed 60% gene suppression at the N/P ratios of 7.5 and 10. Apparently, stearoyl introduction had an optimal stearoylation ratio in the gene suppression tendency. Considering that all the stearoyl PAsp(DET) (12%, 19%, and 32%) had almost the same cellular uptake in 24-hour incubation by flow cytometer measurement (data not shown), 19% stearoyl introduction was the optimal ratio, possibly because of the excellent balance between siRNA release via the intracellular dissociation and sufficient stability of the siRNA complex in the serum-containing media (Fig. 1). It is worth mentioning that none of the tested complexes showed significant gene knockdown when prepared containing EGFP siRNA, suggesting low cytotoxicity and minimal off-target effects of PAsp(DET)-based complexes.

Based on this result, the PAsp(DET)–ST19 complex was further examined for the knockdown ability of a therapeutic gene. VEGF, a well-known regulator of angiogenesis, was selected as the target gene for siRNA knockdown [24]. The endogenous VEGF gene knockdown efficacy of the PAsp(DET)–ST19 complex in Panc-1 cells was compared with two commercially available transfection reagents, Lipofectamine2000 and the linear polyethylenimine-based reagent ExGen500. VEGF mRNA levels were evaluated by real-time PCR (Fig. 3A). The PAsp(DET)–ST19/siRNA complex exhibited around 60% VEGF mRNA reduction, similar to Lipofectamine2000 and much higher than ExGen500 (15% reduction). Furthermore, the amount of VEGF protein secreted from Panc-1 cells was also measured by immunoassay techniques. The VEGF protein production in cells treated with the PAsp(DET)–ST19 complex was also reduced to approximately 50% (Fig. S2).

Another therapeutic gene, anti-apoptotic BCL-2, was also selected to evaluate the potential for future siRNA therapeutics in cancer treatments. The BCL-2 protein has been a common cause of tumor genesis and chemotherapy resistance in various types of tumors [25]. Anti-cancer drug treatment with the reduction of BCL-2 protein expression has been one of the approaches to induce apoptosis in cancer cells [26]. The BCL-2 siRNA sequence used here was selected from a previously published work that indicated this sequence showed high

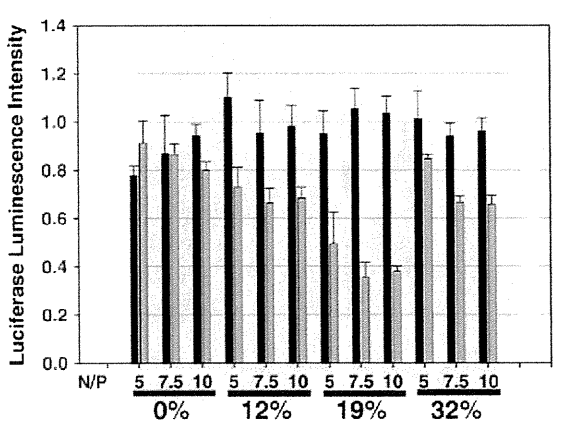

Fig. 2. Luciferase gene knockdown by siRNA complexes of stearoyl PAsp(DET) with different substitution degrees in the B16F10-Luc cell. EGFP siRNA (black) was used as a control for luciferase siRNA (gray). The siRNA complexes were treated at 100 nM concentration for 72-hour incubation. Results are expressed as the mean ± S.D. ($n = 4$).

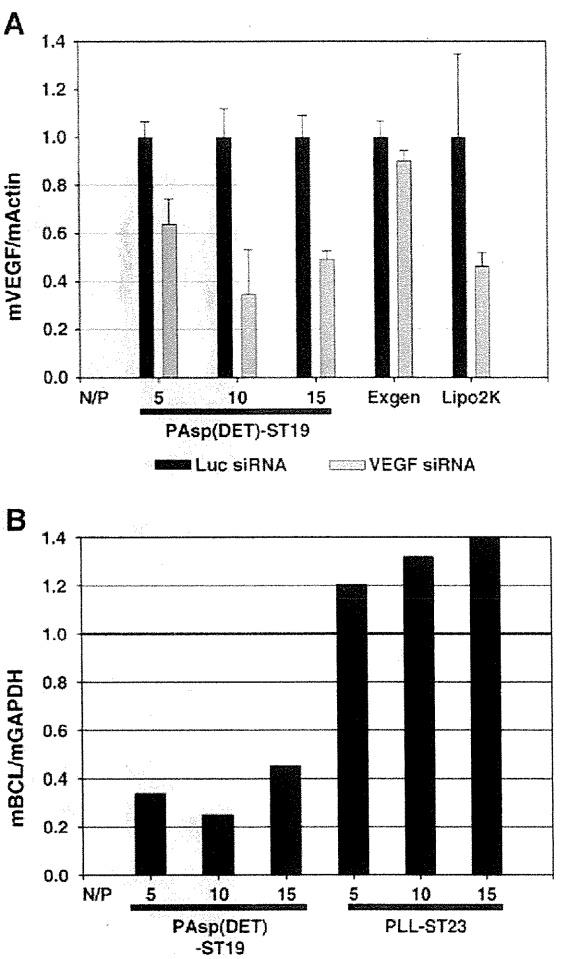

Fig. 3. Endogenous gene knockdown by various siRNA complexes. (A) Comparison of stearoyl PAsp(DET) with ExGen500 and Lipofectamine2000 for endogenous VEGF knockdown by real-time PCR. Each sample was transfected in the Panc-1 cells at 100 nM siRNA concentration for 48 h. The VEGF mRNA amount was normalized with actin mRNA as an internal control. (B) Comparison of stearoyl PAsp(DET) with stearoyl PLL for anti-apoptotic BCL-2 endogenous gene knockdown measured by real-time PCR. Each sample was transfected in the Panc-1 cells for 48 h. The BCL-2 mRNA amount was normalized with GAPDH mRNA as an internal control. In both experiments, luciferase siRNA was used as a control. Results are expressed as the mean ± S.D. ($n = 4$).

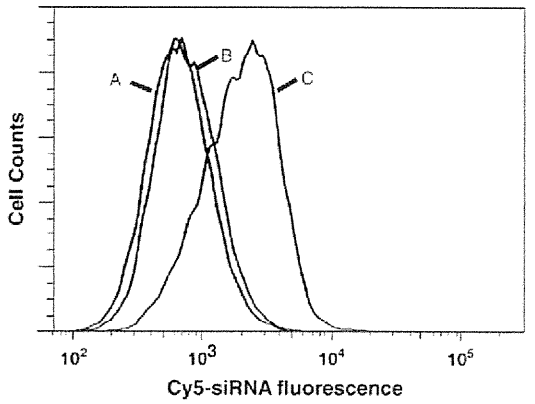

Fig. 4. Cellular uptake of the siRNA complexes in B16F10 cells. Each peak represents the cells treated by naked siRNA (A), unmodified PAsp(DET) (B), and PAsp(DET)–ST19 (C) siRNA complexes (N/P 5.0) from the left.

in vivo gene knockdown efficacy [19]. In this experiment, the PAsp (DET)–ST19 was compared with 23% stearoyl PLL (PLL-ST23) to confirm the backbone superiority for siRNA delivery because PLL is a polycation with poor endosomal escape ability (Fig. 3B). After 48 h of incubation, the BCL-2 mRNA level was evaluated by real-time PCR. The PLL-ST23 showed almost no endogenous gene knockdown or slightly increased BCL-2 expression at the examined N/Ps. On the other hand, gene knockdown was significantly improved with the PAsp(DET)–ST19 complex, with mRNA expression reduced over 60%. The obtained result suggests that the endosomal escaping ability of PAsp(DET) might be crucial for efficient gene knockdown.

3.4. Cellular uptake and intracellular trafficking of stearoyl PAsp(DET)

The transfection results revealed that stearoyl introduction into a PAsp(DET) polymer backbone led to improved siRNA delivery. To elucidate the reason for this improvement, the cellular uptake and intracellular trafficking of the stearoyl PAsp(DET)/siRNA complex were monitored by flow cytometry and CLSM using fluorescence dye-labeled siRNA. B16F10 cells were incubated with naked Cy5-labeled siRNA, Cy5-labeled siRNA complexes of unmodified PAsp(DET) and PAsp(DET)–ST19 for 3 h and analyzed by flow cytometer (Fig. 4). Stearoyl introduction clearly improved the intracellular uptake of siRNA complexes formed with PAsp(DET)–ST19. The uptake of PAsp (DET)–ST19 complex (mean fluorescence 2.3×10^3) was significantly higher than those of unmodified PAsp(DET) complex (8.7×10^2) and naked siRNA (7.4×10^2). This result is probably due to the higher stability of siRNA complexes with stearoyl groups in the cell culture condition (Fig. 1). The uptake of unmodified PAsp(DET) complex was shown to be similar to that of naked siRNA, indicating that cellular

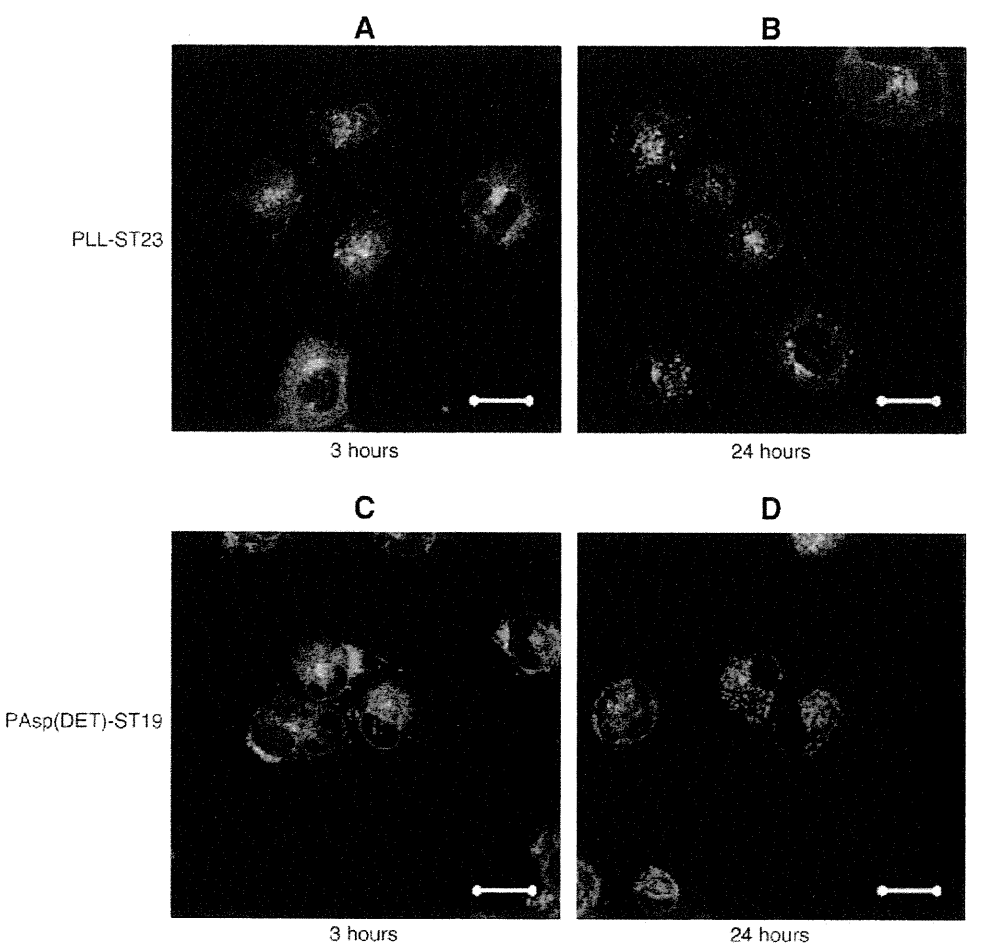

Fig. 5. CLSM images showing intracellular distribution of the siRNA complexes in Panc-1 cells. Panels A and B represent the cells incubated with PLL–ST23 complexes (N/P 5.0) after 3-hour and 24-hour incubations, respectively. Panels C and D represent the cells incubated with PAsp(DET)–ST19 complexes (N/P 5.0) after 3-hour and 24-hour incubations, respectively. Cy3-labeled siRNA and LysoTracker (a late-endosome and lysosome marker) are shown in red and green, respectively. The nucleus was stained with Hoechst 33342 in

uptake of unstable siRNA complex is not efficient. On the other hand, the cellular uptake of PAsp(DET)–ST19 and PLL–ST23 was compared in Panc-1 cells. Although the PLL–ST23 complex showed no gene knockdown in Fig. 3B, it (1.3×10^4) was internalized more efficiently than the PAsp(DET)–ST19 complex (1.0×10^4) (data not shown), indicating that steps following internalization, such as endosome escape, are crucial for siRNA-mediated gene knockdown.

The endosome escape behavior of the PAsp(DET)–ST19 complex was compared with that of the PLL–ST23 complex by CLSM observation in Panc-1 cells (Fig. 5). The siRNA was labeled with Cy3 (red), and late-endosomes and lysosomes were stained with LysoTracker Green (green). Nuclei were stained with Hoechst 33342 (blue). Cy3-labeled siRNA colocalized in late-endosomes and lysosomes should be shown as yellow, and endosomal escape of the siRNA would induce the recovery of red color from yellow over time. After 3-hour incubation, Cy3-labeled siRNA of the PLL–ST23 complex was observed mainly in the cell interior with yellow fluorescence and localized in small confined spaces (Fig. 5A), indicating that the majority of Cy3-labeled siRNA was trapped in late-endosomes/lysosomes and only a small portion of the complex escaped from the organelles. Even after 24-hour incubation (Fig. 5B), very little red fluorescence was observed in the cytoplasm, whereas large yellow regions were still observed, indicating that the major stearoyl PLL complexes were still trapped in the late-endosome/lysosome compartments. In contrast, the PAsp (DET)–ST19 complex exhibited some red fluorescence surrounding yellow late-endosomes/lysosomes even after only 3-hour incubation (Fig. 5C). The observation in 24-hour incubation (Fig. 5D) showed that red and green fluorescence were separated in the cytoplasm with almost no yellow fluorescence, demonstrating the ability of the stearoyl PAsp(DET) to decrease the amount of siRNA molecules trapped in the late-endosomes/lysosomes.

The detailed colocalization profile was further analyzed using ImageJ software, which calculates Spearman's rank correlation coefficient from the red and green channels of the confocal images [21]. The coefficient value ranges from −1 to 1, where 0 indicates that there is no discernable correlation and −1 and +1 mean strong negative and positive correlations, respectively. The correlation coefficient value for the PLL–ST23 complex of the 24-hour incubation was 0.72, which means there was a strong positive correlation between the distribution of red and green fluorescence. In contrast, the correlation coefficient value of the PAsp(DET)–ST19 complex after 24-hour incubation was calculated to be 0.23, indicating little discernable correlation between Cy3-siRNA and late-endosomes/lysosomes. The obtained correlation values quantitatively confirm that stearoyl PAsp (DET) significantly decreased the amount of siRNA complexes trapped in late-endosomes/lysosomes. This stronger endosome escape ability is likely responsible for the enhanced siRNA transfection compared to stearoyl PLL. The outstanding endosome escape ability of stearoyl PAsp(DET) is considered to be mainly due to the pH-dependent protonation of *N*-(2-aminoethyl)-2-aminoethyl groups in the PAsp(DET) side chain [7]. Consequently, the enhanced gene suppression efficacy of the PAsp(DET)–ST19 appears to be based on the higher cellular uptake and efficient endosomal escape (Fig. 4).

3.5. *Cell viability of stearoyl PAsp(DET)*

Low cytotoxicity as well as high knockdown efficacy is critical factors for the development of an effective siRNA carrier. Therefore, cell viability after introduction of stearoyl PAsp(DET)/siRNA complexes was measured by the MTT assay in Panc-1 cells (Fig. 6). The obtained cell viability was over 90% for each stearoyl PAsp(DET) complex, similar to ExGen500 and higher than Lipofectamine 2000 (approximately 80% cell viability), indicating the minimal cytotoxicity of the stearoyl PAsp(DET) complexes in this experimental condition.

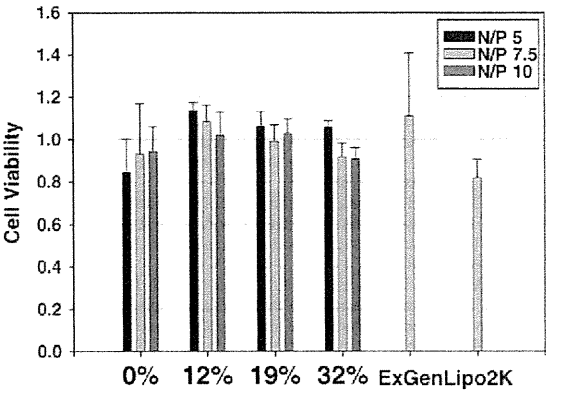

Fig. 6. Viability of Panc-1 cells treated with each siRNA complex under the same experimental condition as the real-time PCR. Results are expressed as the mean ± S.D. ($n = 4$).

4. Conclusion

In this study, we demonstrated that stearoyl introduction onto PAsp(DET) side chains led to the formation of a siRNA complex with improved *in vitro* RNAi activity. Stearoyl introduction significantly enhanced the cellular uptake of siRNA due to complex stabilization via hydrophobic interaction. Additionally, the PAsp(DET) polycation backbone contributed to the excellent endosomal escape of siRNA complexes. Ultimately, the PAsp(DET)–ST19 complexes formed at N/Ps of 7.5–10 exhibited the best combination of high RNAi activity with low cytotoxicity of the tested samples, including commercially available reagents. The stearoyl PAsp(DET)/siRNA complex is a promising candidate for therapeutic siRNA delivery, a result of rational carrier design aimed to overcome specific subcellular barriers.

Acknowledgements

This work was financially supported by a Core Research for Evolutional Science and Technology (CREST) grant from the Japan Science and Technology Agency (JST) as well as Takeda Science Foundation. HJ Kim is thankful to Mr. Kazuya Suma for his help with the polymer synthesis.

Appendix A. Supplementary data

Supplementary data associated with this article can be found, in the online version, at doi: 10.1016/j.jconrel.2010.03.019.

References

[1] L. Aagaard, J.J. Rossi, RNAi therapeutics: principles, prospects and challenges, Adv. Drug Deliv. Rev. 59 (2007) 75–86.
[2] D.R. Corey, Chemical modification: the key to clinical application of RNA interference? J. Clin. Invest. 117 (2007) 3615–3622.
[3] D.A. Braasch, Z. Paroo, A. Constantinescu, G. Ren, O.K. Öz, R.P. Mason, D.R. Corey, Biodistribution of phosphodiester and phosphorothioate siRNA, Bioorg. Med. Chem. Lett. 14 (2004) 1139–1143.
[4] A. Akinc, A. Zumbuehl, M. Goldberg, E.S. Leshchiner, V. Busini, N. Hossain, S.A. Bacallado, D.N. Nguyen, J. Fuller, R. Alvarez, A. Borodovsky, T. Borland, R. Constien, A. de Fougerolles, J.R. Dorkin, K.N. Jayaprakash, M. Jayaraman, M. John, V. Koteliansky, M. Manoharan, L. Nechev, J. Qin, T. Racie, D. Raitcheva, K.G. Rajeev, D.W.Y. Sah, J. Soutschek, I. Toudjarska, H.-P. Vornlocher, T.S. Zimmermann, R. Langer, D.G. Anderson, A combinatorial library of lipid-like materials for delivery of RNAi therapeutics, Nat. Biotechnol. 26 (2008) 561–569.
[5] H. de Martimprey, C. Vauthier, C. Malvy, P. Couvreur, Polymer nanocarriers for the delivery of small fragments of nucleic acids: oligonucleotides and siRNA, Eur. J. Pharm. Biopharm. 71 (2009) 490–504.
[6] M. Neu, D. Fischer, T. Kissel, Recent advances in rational gene transfer vector design based on poly(ethylene imine) and its derivatives, J. Gene Med. 7 (2005) 992–1009.
[7] K. Miyata, M. Oba, M. Nakanishi, S. Fukushima, Y. Yamasaki, H. Koyama, N. Nishiyama, K. Kataoka, Polyplexes from poly(aspartamide) bearing 1, 2-diaminoethane side

chains induce pH-selective, endosomal membrane destabilization with amplified transfection and negligible cytotoxicity, J. Am. Chem. Soc. 130 (2008) 16287–16294.
[8] N. Kanayama, S. Fukushima, N. Nishiyama, K. Itaka, W.-D. Jang, K. Miyata, Y. Yamasaki, U.-I. Chung, K. Kataoka, A PEG-based biocompatible block catiomer with high buffering capacity for the construction of polyplex micelles showing efficient gene transfer toward primary cells, ChemMedChem 1 (2006) 439–444.
[9] K. Masago, K. Itaka, N. Nishiyama, U.-I. Chung, K. Kataoka, Gene delivery with biocompatible cationic polymer: pharmacogenomic analysis on cell bioactivity, Biomaterials 28 (2007) 5169–5179.
[10] D. Akagi, M. Oba, H. Koyama, N. Nishiyama, S. Fukushima, T. Miyata, H. Nagawa, K. Kayaoka, Biocompatible micellar nanovectors achieve efficient gene transfer to vascular lesions without cytotoxicity and thrombus formation, Gene Ther. 14 (2007) 1029–1038.
[11] M. Harada-Shiba, I. Takamisawa, K. Miyata, T. Ishii, N. Nishiyama, K. Itaka, K. Kangawa, F. Yoshihara, Y. Asada, K. Hatakeyama, N. Nagaya, K. Kataoka, Intratracheal gene transfer of adrenomedullin using polyplex nanomicelles attenuates monocrotaline-induced pulmonary hypertension in rats, Mol. Ther. 17 (2009) 1180–1186.
[12] K. Miyata, M. Oba, M.R. Kano, S. Fukushima, Y. Vachutinsky, M. Han, H. Koyama, K. Miyazono, N. Nishiyama, K. Kataoka, Polyplex micelles from triblock copolymers composed of tandemly aligned segments with biocompatible, endosomal escaping, and DNA-condensing functions for systemic gene delivery to pancreatic tumor tissue, Pharm. Res. 25 (2008) 2924–2936.
[13] K. Itaka, S. Ohba, K. Miyata, H. Kawaguchi, K. Nakamura, T. Takato, U.-I. Chung, K. Kataoka, Bone regeneration by regulated in vivo gene transfer using biocompatible polyplex nanomicelles, Mol. Ther. 15 (2007) 1655–1662.
[14] S.C. de Smedt, J. Demeester, W.E. Hennink, Cationic polymer based gene delivery systems, Pharm. Res. 17 (2000) 113–126.
[15] Y. Wang, S. Gao, W.-H. Ye, H.S. Yoon, Y.-Y. Yang, Co-delivery of drugs and DNA from cationic core-shell nanoparticles self-assembled from a biodegradable copolymer, Nat. Mater. 5 (2006) 791–796.
[16] A. Alshamsan, A. Haddadi, V. Incani, J. Samuel, A. Lavasanifar, H. Uludag, Formulation and delivery of siRNA by oleic acid and stearic acid modified polyethylenimine, Mol. Pharm. 6 (2009) 121–133.
[17] W.J. Kim, L.V. Christensen, S. Jo, J.W. Yockman, J.H. Jeong, Y. -H. Kim, S. W. Kim, Cholesteryl oligoarginine delivering vascular endothelial growth factor siRNA effectively inhibits tumor growth in colon adenocarcinoma, Mol. Ther. 14 (2006) 343–350.
[18] A. Harada, K. Kataoka, Formation of polyion complex micelles in an aqueous milieu from a pair of oppositely-charged block copolymers with poly(ethylene glycol) segments, Macromol. 28 (1995) 5294–5299.
[19] M. Ocker, D. Neureiter, M. Lueders, S. Zopf, M. Ganslmayer, E.G. Hahn, C. Herold, D. Schuppan, Variants of bcl-2 specific siRNA for silencing antiapoptotic bcl-2 in pancreatic cancer, Gut 54 (2005) 1298–1308.
[20] K. de Bruin, N. Ruthardt, K. von Gersdorff, R. Bausinger, E. Wagner, M. Ogris, C. Bräuchle, Cellular dynamics of EGF receptor-targeted synthetic viruses, Mol. Ther. 15 (2007) 1297–1305.
[21] A.P. French, S. Mills, R. Swarup, M.J. Bennett, T.P. Pridmore, Colocalization of fluorescent markers in confocal microscope images of plant cells, Nat. Protoc. 3 (2008) 619–628.
[22] M. Meyer, A. Philipp, R. Oskuee, C. Schmidt, E. Wagner, Breathing life into polycations: functionalization with pH-responsive endosomolytic peptides and polyethylene glycol enables siRNA delivery, J. Am. Chem. Soc. 130 (2008) 3272–3273.
[23] J. DeRouchey, C. Schmidt, G.F. Walker, C. Koch, C. Plank, E. Wagner, J.O. Rädler, Monomolecular assembly of siRNA and poly(ethylene glycol)-peptide copolymers, Biomacromolecules 9 (2008) 724–732.
[24] L.M. Ellis, D.J. Hicklin, VEGF-targeted therapy: mechanisms of anti-tumour activity, Nat. Rev. Cancer 8 (2008) 579–591.
[25] D.S. Ziegler, A.L. Kung, Therapeutic targeting of apoptosis pathways in cancer, Curr. Opin. Oncol. 20 (2008) 97–103.
[26] J. George, N.L. Banik, S.K. Ray, Bcl-2 siRNA augments taxol mediated apoptotic death in human glioblastoma U138MG and U251MG cells, Neurochem. Res. 34 (2009) 66–78.

Biomaterials 31 (2010) 3707–3714

Contents lists available at ScienceDirect

Biomaterials

journal homepage: www.elsevier.com/locate/biomaterials

Biodegradable polyamino acid-based polycations as safe and effective gene carrier minimizing cumulative toxicity

Keiji Itaka [a,d,1], Takehiko Ishii [b,d,1], Yoko Hasegawa [a,d], Kazunori Kataoka [a,b,c,d,*]

[a] Division of Clinical Biotechnology, Center for Disease Biology and Integrative Medicine, Graduate School of Medicine, The University of Tokyo, 7-3-1 Hongo, Bunkyo-ku, Tokyo 113-0033, Japan
[b] Department of Bioengineering, Graduate School of Engineering, The University of Tokyo, 7-3-1 Hongo, Bunkyo-ku, Tokyo 113-0033, Japan
[c] Department of Materials Science and Engineering, Graduate School of Engineering, The University of Tokyo, 7-3-1 Hongo, Bunkyo-ku, Tokyo 113-0033, Japan
[d] Center for NanoBio Integration, The University of Tokyo, 7-3-1 Hongo, Bunkyo-ku, Tokyo 113-0033, Japan

ARTICLE INFO

Article history:
Received 4 November 2009
Accepted 23 November 2009
Available online 13 February 2010

Keywords:
Non-viral gene carrier
Cationic polymer
Biodegradable polycation
Polyplex
Cumulative toxicity

ABSTRACT

Gene delivery using cationic polymers has attracted much attention due to their potential advantages, such as large DNA loading capacity, ease of large-scale production, and reduced immunogenicity. We recently reported that polyplexes from poly[N-[N-(2-aminoethyl)-2-aminoethyl]aspartamide] (P[Asp(DET)]), having an efficient endosomal escape due to pH-selective membrane destabilization, showed high transfection efficiency with minimal toxicity. Pharmacogenomic analysis demonstrated that P[Asp(DET)] also provided long-term security after transfection. We hypothesized that the biodegradability of P[Asp(DET)] played a significant role in achieving effective transfection. Gel permeation chromatography (GPC) and electrospray ionization mass spectrometry (ESI-MS) measurements of P[Asp(DET)] revealed their ability to undergo rapid degradation. In contrast, a derivative polycation, N-substituted polyglutamide (P[Glu(DET)]), showed no degradability, indicating that the degradation of P[Asp(DET)] was induced by a specific self-catalytic reaction between the PAsp backbone and the side-chain amide nitrogen. Degradation products of P[Asp(DET)] caused no cytotoxicity, even at high concentrations in the culture medium. Repeated transfection by administering the polyplexes for every 24 h showed that biodegradable P[Asp(DET)] provided a continuous increase in transgene expression, while non-degradable P[Glu(DET)] showed a decrease in transgene expression after 48 h, coupled with fluctuations in expression profiles of endogenous genes. *In vivo* intraperitoneal injection of P[Asp(DET)] induced minimal inflammatory cytokine induction to a level comparable to that of normal saline. These results indicate that the biodegradability of P[Asp(DET)] played a key role in achieving safe and sustained transgene expression, by minimizing cumulative toxicity caused by polycations remaining in cells or in the body.

1. Introduction

Applications of gene therapy have been considered in many clinical fields. Safe and efficient gene introduction are prerequisites for successful gene therapy. During the past decade, various cationic polymers have attracted much attention for use as non-viral gene carriers, as they have many potential advantages, such as large DNA loading capacity, ease of large-scale production, and reduced immunogenicity that has been an issue associated with the use of viral vectors [1–3].

Among these polymers, polyethylenimine (PEI) and its derivatives have been extensively investigated due to their excellent transfection efficiencies [4]. However, their clinical use has been limited primarily due to their toxicities. We recently found a flanking benzyl ester group of poly(β-benzyl L-aspartate) (PBLA) that underwent a quantitative aminolysis reaction with a variety of amine compounds under very mild condition. Using this reaction, we prepared an N-substituted poly(aspartamide) (PAsp) derivative library possessing a variety of cationic side chains from a single PBLA platform. Through a series of transfection and cytotoxicity assays using this library, a highly promising candidate, poly[N-[N-(2-aminoethyl)-2-aminoethyl]aspartamide] (P[Asp(DET)]) was emerged to show high capacity with minimal toxicity (Fig. 1) [5].

* Corresponding author at: Department of Materials Engineering, Graduate School of Engineering, The University of Tokyo, 7-3-1 Hongo, Bunkyo-ku, Tokyo 113-0033, Japan. Tel.: +81 3 5841 7138; fax: +81 3 5841 7139.
E-mail address: kataoka@bmw.t.u-tokyo.ac.jp (K. Kataoka).
[1] The first two authors contributed equally to this work.

0142-9612/$ – see front matter © 2009 Elsevier Ltd. All rights reserved.
doi:10.1016/j.biomaterials.2009.11.072

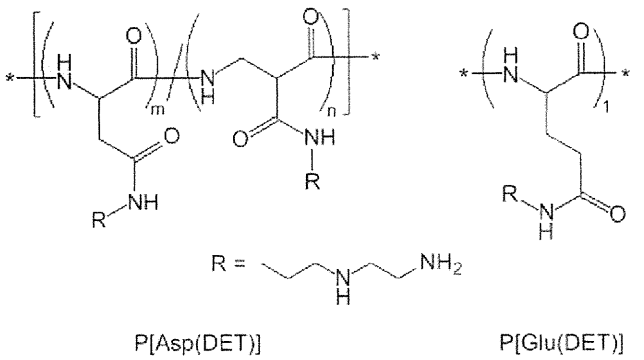

Fig. 1. Molecular structures of P[Asp(DET)] and P[Glu(DET)].

P[Asp(DET)] showed an excellent transgene expression comparable to a commercially available linear PEI (ExGen 500) and a lipid-based system (LipofectAMINE 2000) [6]. By the form of PEGylated polyplexes (polyplex micelle; poly(ethylene glycol) (PEG)-P[Asp(DET)] block copolymer/pDNA), we have successfully introduced the transgene into aminal models, such as (i) a rabbit's clamped carotid artery with neointima via intra-arterial injection 15 [7], (ii) a mouse skull by regulated release from a calcium phosphate cement scaffold to induce bone regeneration through differentiation factor transduction [8], and (iii) a mouse lung via intratracheal administration to cure pulmonary hypertension by introducing the adrenomedullin gene [9].

Safe and efficient gene introduction using (PEG-)P[Asp(DET)] has been attributed to its unique 1,2-diaminoethane side chain, where the N-(2-aminoethyl)-2-aminoethyl group exhibits a distinctive two-step protonation behavior [5]. This dual protonation state suggests that strong pH-buffering capacity of P[Asp(DET)] units was responsible for an efficient endosomal escape, which has often been explained as the mechanism underlying the excellent transfection efficiency of PEI. In addition, we recently found that pH-selective membrane destabilization by P[Asp(DET)] played a key role in an efficient endosomal escape of P[Asp(DET)]/DNA polyplexes into the cytoplasm [10]. The reduced cytotoxicity caused by P[Asp(DET)] was attributed with its limited interactions with other plasma and cytoplasmic membranes at neutral pH.

Another important aspect in achieving a good therapeutic effect is the long-term security of the polymers. We have already shown that, when used in application with primary cells, P[Asp(DET)] induces cell differentiation more effectively than that by other commercially available reagents [8]. Pharmacogenomic analysis suggested that P[Asp(DET)] maintained cellular homeostasis after transfection [6]. Although comparable reporter gene expression and cell viability were obtained after a few days of transfection, the efficacy of inducing cell differentiation differed significantly among the reagents. The carrier materials complexed with DNA inevitably remain within cells after releasing the DNA, either in the cytoplasm or nucleus. Thus, it is reasonable to assume that the safety of the polymers remaining within cells may significantly affect cell behavior.

For this study, we hypothesized that this aspect of safety would be strongly attributed to the biodegradability of P[Asp(DET)]. We compared the physicochemical properties underlying the degradability of P[Asp(DET)] with that of a non-degradable derivative polymer. Sustained transgene expression and cell viability were demonstrated with *in vitro* assays using cultured cells. Finally, cytokine induction after *in vivo* administration of polymers was determined to evaluate the feasibility of therapeutic uses of these polymers.

2. Materials and methods

2.1. Materials

β-benzyl-L-aspartate N-carboxy-anhydride (BLA-NCA) was synthesized according to Fuchs' method. N-Methyl-2-pyrrolidone (NMP) was purchased from Nacalai tesque Inc. (Kyoto, Japan). *n*-Buthylamine, benzene, N,N-dimethylformamide (DMF) and dichloromethane (CH_2Cl_2) were purchased from Wako Pure Chemical Industries, Ltd. (Osaka, Japan). 2-Hydroxypyridine was purchased from Aldrich Chem. Co. (Milwaukee, WI, USA), distilled under reduced pressure, and recrystalized from ethanol. Diethylenetriamine (DET) was purchased from Tokyo Chemical Industry (Tokyo, Japan). For chemical reactions, *n*-buthylamine, DET, and NMP were distilled from calcium hydride (CaH_2) under reduced pressure. DMF and CH_2Cl_2 were purified by passing through two packed columns of neutral alumina (Glass Contour, Irvine, CA, USA).

Plasmid DNAs (pDNA) encoding firefly luciferase (pGL4.13: Promega, Madison, WI, USA) and renilla luciferase (pRL-CMV: Promega) were amplified in competent DH5α Escherichia coli and purified using NucleoBond Xtra EF (Nippon Genetics, Tokyo, Japan). The pDNA concentration was determined from the absorbance at 260 nm. Dulbecco's modified Eagle's medium (DMEM) and fetal bovine serum (FBS) were purchased from Sigma–Aldrich (St. Louis, MO, USA) and Life Technologies Japan Ltd. (Tokyo, Japan), respectively. Linear polyethylenimine (LPEI) (Exgen 500, MW = 22 kDa) was purchased from MBI Fermentas (Burlington, ON, Canada). Lipopolysaccharide (LPS: L4391) was purchased from Sigma–Aldrich.

2.2. Cells and animals

Human hepatoma cells (HuH-7) and human umbilical vein endothelial cells (HUVEC) were obtained from the Japanese Collection of Research Bioresources Cell Bank (Tokyo, Japan) and Lonza Ltd. (Basel, Switzerland), respectively. Bioluminescent cells (HuH-7-luc) stably expressing firefly luciferase were kindly provided by Mr. S. Matsumoto (The University of Tokyo).

Female ICR mice were purchased from Charles River Laboratories (Tokyo, Japan). All animal experimental protocols were performed in accordance with the guidelines of the Animal Committee of the University of Tokyo.

2.3. Preparation of poly(β-benzyl-L-aspartate) (PBLA) and poly(γ-benzyl-L-glutamate) (PBLG)

To obtain PBLA, BLA-NCA (1.2 g, 5 mmol) was dissolved in DMF (2 mL), diluted with CH_2Cl_2 (20 mL), and *n*-butylamine (10-fold dilution with CH_2Cl_2, 0.045 mL, 0.045 mmol) was added to initiate the ring-opening polymerization of NCA. The reaction solution was stirred for two days at 35 °C. All these procedures were performed under an argon atmosphere. PBLA was recovered by precipitation in an excess amount of *n*-hexane/AcOEt (6:4), and the filtrate was dried in vacuo. PBLG was prepared in a similar manner, except using BLG-NCA as a monomer. PBLA and PBLG obtained were analyzed at 40 °C using a gel permeation chromatography (GPC) system (TOHSO HLC-8220, Japan) equipped with TSK-gel Super AW4000 and Super AW3000 × 2 in series, as well as an internal refractive index (RI) detector, and confirmed to be unimodal with narrow distribution (M_w/M_n = 1.06 and 1.11, respectively). NMP containing 50 mM lithium bromide was used as an eluent. PEG standards were used to calibrate the molecular weight and the molecular weight distribution. From the ^{1}H nuclear magnetic resonance (NMR) spectra of PBLA and PBLG, their polymerization degrees were confirmed to be 102 and 89, respectively (d_6-DMSO at 80 °C, Supplemental Fig. S1).

2.4. Preparation of N-substituted polyaspartamide, P[Asp(DET)]

N-substituted polyaspartamides were prepared through the aminolysis reaction of PBLA. Lyophilized PBLA (50 mg) was dissolved in NMP (2 mL), and cooled to 0 °C. In another reaction tube, DET (50-fold excess molar to the benzyl ester units) was diluted twice with NMP, and cooled at 0 °C. The PBLA solution was added dropwise into the DET solution. After 1 h of reaction, the reaction mixture was added dropwise into a well-chilled 5 N HCl aqueous solution (equimolar amount to the added amino groups), where the temperature was kept below 10 °C. Then the mixture was first dialyzed against an aqueous solution of 0.01 N HCl and then against de-ionized water at 4 °C in a dialysis tube (MWCO: 6-8000). The final solution was lyophilized, and objective P[Asp(DET)] was obtained as the chloride salt form with a good yield. Quantitative introduction of DET was confirmed by ^{1}H NMR spectrum (Supplemental Fig. S2).

2.5. Preparation of N-substituted polyglutamide, P[Glu(DET)]

The ester-amide exchange reaction of PBLG was performed using DET in the presence of 2-hydroxypyridine as a catalyst according to the literature [11]. PBLG (0.2 g, 0.95 mmol) and 2-hydoxypyridine (452 mg, 5 eq.) were dissolved in DMF (4 mL), followed by the addition of DET (2 mL, 20-fold molar excess of benzyl ester units). After stirring the mixture for 30 h at 25 °C, it was treated in a similar manner with polyaspartamides as described above. Due to a small amount of undesirable

side reactions, such as cross-linking, additional purification was performed using a fractional preparative GPC system equipped with Superdex 200 pg XK50/60 column (GE healthcare, UK) and UV detector set at 220 nm. Phosphate buffer solution (10 mM, pH 7.4) containing 0.5 M NaCl was used as an eluent at a flow rate of 15 mL/min at room temperature. The main peak fractions were combined and dialyzed first against an aqueous solution of 0.01 N HCl, and then against de-ionized water at 4 °C. The final solution was lyophilized, and P[Glu(DET)] was obtained in the chloride salt form. Quantitative introduction of DET was confirmed by ^{1}H NMR spectrum (Supplemental Fig. S2).

2.6. Time-course GPC measurements

Time-course degradation profiles of P[Asp(DET)] and P[Glu(DET)] were evaluated using a GPC system (Jasco, Tokyo, Japan) equipped with Superdex 75 10/300 GL column (GE Healthcare UK, Ltd.) and UV detector set at 220 nm. Phosphate buffer solution (10 mM) containing 0.5 M NaCl was used as an eluent at a flow rate of 0.75 mL/min at room temperature. All samples were dissolved in citrate buffer (pH 3.0), acetate buffer (pH 5.5), phosphate buffer (pH 7.4), or carbonate buffer (pH 9.0) solution containing 0.15 M NaCl. These were stored at 4 °C, 25 °C, and 37 °C and analyzed at defined time points.

2.7. Electrospray ionization mass spectrometry (ESI-MS) measurements

P[Asp(DET)] (5 mg) was dissolved in Milli-Q water (5 mL) adjusting the pH to 7.4, sterilized by filtration (0.1 μm pore size), and incubated at 37 °C for one month. ESI-MS (AccuoTOF, JEOL, Tokyo, JAPAN) was conducted in the positive ion mode with an atmospheric pressure ionization electrospray interface, flushed with heated dry nitrogen gas (heater temperature 250 °C) at a constant flow rate of 10 L/min. The sample was diluted with methanol and injected at a constant flow rate of 0.1 mL/min. The spectrometer scanned from *m/z* 130 to 500.

2.8. Evaluation of cell viability after addition of polymers to the culture medium

HuH-7 or HUVEC cells were seeded in 96-well culture plates (HuH-7: 4000 cells/well, HUVEC: 5000 cells/well) and incubated overnight in 100 μL DMEM supplemented with 10% FBS and penicillin/streptomycin. After the culture medium was replaced with fresh medium containing 10% FBS, a polymer solution of P[Asp(DET)], P[Glu(DET)], LPEI or the degradation products P[Asp(DET)] obtained after incubation at 37 °C were added at varing concentration. Cell viability was determined using the Cell Counting Kit-8 (Dojindo, Kumamoto, Japan) following the manufacturer's protocol.

2.9. Polyplex formation

Each polyplex sample with a pDNA concentration of 33 μg/mL was prepared by mixing pDNA and polycation (P[Asp(DET)], P[Glu(DET)] or LPEI) at the indicated N/P ratio (=[total amines in polycation]/[DNA phosphates]) in Tris–HCl buffer solution (10 mM, pH 7.4).

2.10. Luciferase expression after transfection using polyplexes

Cells were seeded in 96-well culture plates and incubated overnight in 100 μL DMEM supplemented with 10% FBS and penicillin/streptomycin. For each transfection, the culture medium was replaced with fresh medium containing 10% FBS and then the polyplex solution was administered to each well. Firefly luciferase expression was measured with the Luciferase assay system (Promega, Madison, WI, USA) and a GloMaxTM 96 microplate luminometer (Promega) according to the manufacturer's protocol. Luciferase expressions of firefly and renilla were measured with the Dual-luciferase reporter assay system (Promega).

2.11. Housekeeping gene expression assay

After performing a similar transfection procedure as previously described, total RNA was collected after 48 h using an RNeasy Mini Preparation Kit (Qiagen, Hilden, Germany). Taqman express endogenous control plate (Applied Biosystems, Foster City, CA, USA) was used to evaluate the expression of 31 endogenous housekeeping genes and 18S rRNA. The expression of each gene was normalized by the expression of 18S rRNA, and the data were expressed as relative values to the control cells without transfection.

2.12. Evaluation of cytokine induction after in vivo administration of polymers

Mice were anesthetized with isoflurane inhalation, and then 300 μL of polymer solution containing 0.79 μmol amine was injected intraperitoneally. This amine dose corresponded to that used for complexing 50 μg pDNA. After 4 h of injection, the whole blood was collected from inferior vena cava and left overnight at 4 °C. Samples were centrifuged and the supernatants were harvested for serum. Serum concentrations of IL-6 and TNF-α were measured by Quantikine colorimetric sandwich ELISA kits (R&D Systems, Minneapolis, MN, USA), following the manufacturer's instructions.

3. Results

3.1. Biodegradability of P[Asp(DET)] and P[Glu(DET)]

To evaluate the biodegradability of P[Asp(DET)], GPC measurements were performed after incubating P[Asp(DET)] (pH 7.4) at 37 °C. As shown in Fig. 2A, P[Asp(DET)] showed considerable degradation even after one-day incubation which progressed gradually. When the degradation products formed in the solution at pH 7.4 were analyzed by ESI-MS, most of the detectable signals were in good agreement with masses of Asp(DET) monomer and its oligomers (Fig. 3). This suggested that degradation occurred due to selective backbone cleavage of P[Asp(DET)].

The facile degradability of N-substituted polyaspartamides has been previously reported, although the exact mechanism remained unclear [12]. An asparagine (Asn) residue in peptides and proteins is known to induce non-enzymatic deamidation under physiological conditions, which results in the rearrangement of Asn to Asp while releasing NH_3 [13–17]. In this reaction, five-member succinimide intermediate formation plays an important role [14].

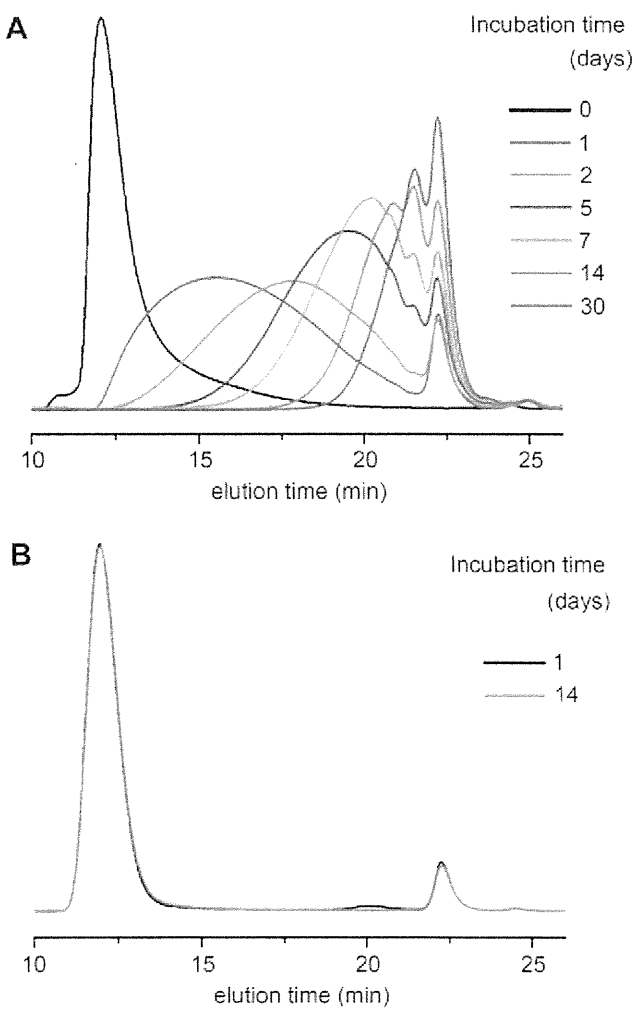

Fig. 2. GPC profiles during time-course degradation of P[Asp(DET)] (A) and P[Glu(DET)] (B) in phosphate buffer solution (10 mM, pH 7.4) containing 150 mM NaCl at 37 °C.

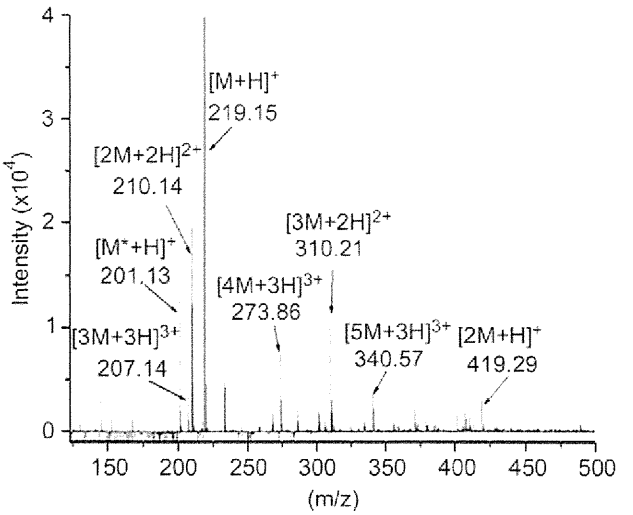

Fig. 3. ESI-MS spectrum of degraded P[Asp(DET)]. The sample was incubated as an aqueous solution (pH 7) at 37 °C for one month. M: estimated molecular mass of Asp(DET) and isomerized Asp(DET), M*: estimated molecular mass of Asp(DET) as a five-membered ring intermediate.

Although succinimide formation of Asn primarily occurs via a nucleophilic attack of the amide nitrogen backbone on the side-chain carbonyl (Fig. 4 pathway (a)), cleavage of the backbone at an Asn residue in peptides and proteins has also been reported, where succinimide formation occurred via a nucleophilic attack of a side-chain amide nitrogen on the backbone carbonyl (Fig. 4 pathway (b)) [13,15,17]. Thus, it is reasonable to assume that five-membered succinimide formation played an important role in the cleavage of the PAsp backbone.

Then, we synthesized a derivative polymer, N-substituted polyglutamide (P[Glu(DET)]), as a comparative gene carrier (Fig. 1). Although an N-substituted polyglutamide can also form a six-membered cyclic imide in similar mechanism as P[Asp(DET)], the conformation has less favorable geometry [15,18]. As expected, P[Glu(DET)] showed no degradation, even after a two-week incubation at 37 °C (Fig. 2B). It should be noted that these two polymers possess an identical DET side chain, which has been shown to have an excellent gene transfection efficiency, as described in the Introduction section. Thus, by comparing these two polymers, we could analyze the biological functions specifically related to the degradabilities of these polymers.

3.2. Polymer degradability in maintaining cellular homeostasis

We hypothesized that degradability of a polymer would play an important role in achieving safe and sustained transgene expression. First, we evaluated cell viability in the presence of polymers in the culture medium. The intact polymer of P[Asp(DET)], P[Glu(-DET)], LPEI, or the degradation products of P[Asp(DET)] were added to the culture medium at varying concentrations. As shown in Fig. 5, the intact polymers showed cytotoxicity in a manner dependent on the concentration of amines, where an amine concentration of >0.04 mM (HuH-7) or 0.01 mM (HUVEC) resulted in decreased cell viability. In contrast, the degradation products of P[Asp(DET)] collected after incubation at 37 °C resulted in less cytotoxicity. In particular, using the degradation products after incubation for two or more days, no cytotoxicity was evident, even at high concentrations of amines (up to 1 mM).

Next, we evaluated the transfection efficiency of cultured cells. To focus on cell conditions and transgene expression, we used HuH-7 cells that stably expressed firefly luciferase and evaluated the fluctuations in endogenous firefly expression and transfected renilla luciferase expression. In preliminary experiments, transfection with single administration of polyplexes followed by the

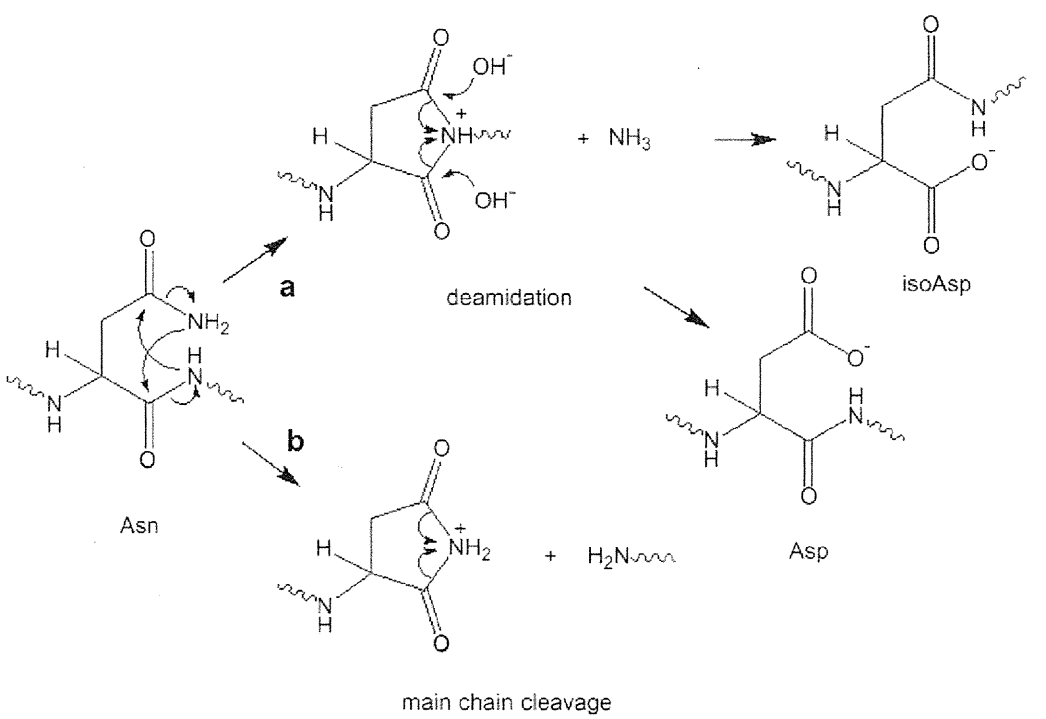

Fig. 4. Pathway for spontaneous deamidation of Asn, followed by isomerization of Asp (a) and backbone cleavage by an asparagine residue in polypeptides (b).

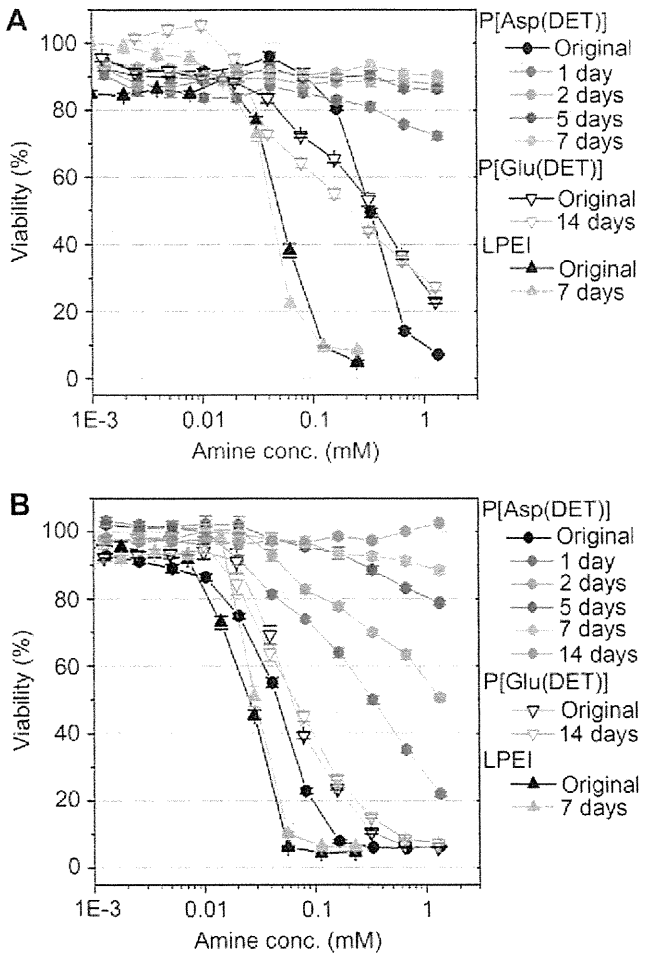

Fig. 5. Cell viability after addition of P[Asp(DET)], P[Glu(DET)], LPEI, or the degradation products of P[Asp(DET)]. HuH-7 (A) or HUVEC (B) cells were incubated in the presence of these compounds at varying concentrations and their viabilities were evaluated after 48 h.

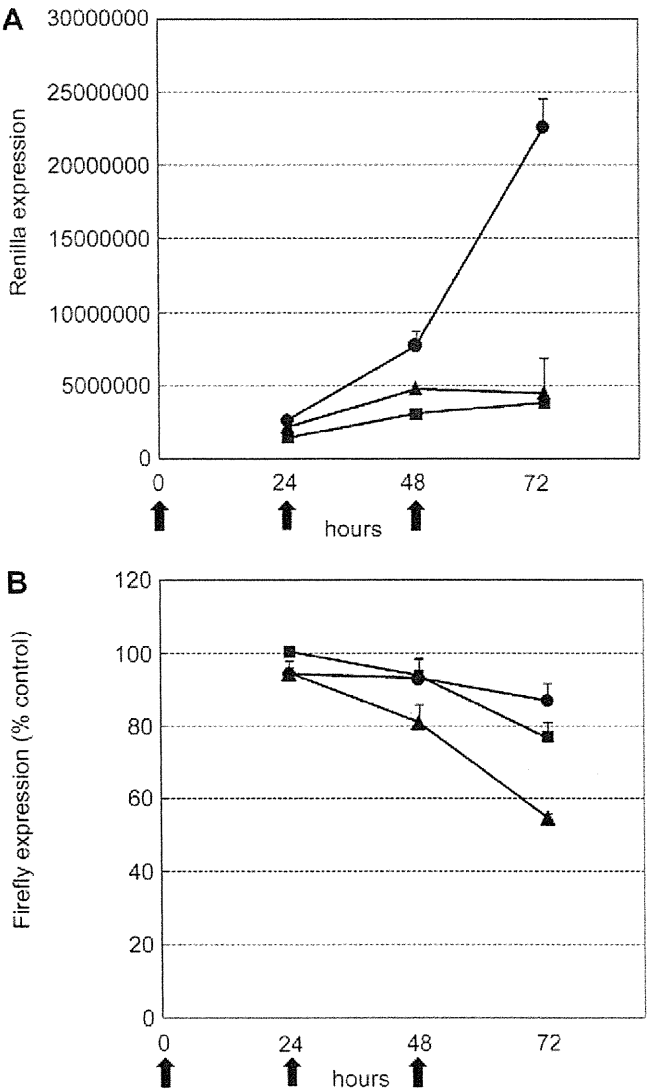

Fig. 6. Repeated transfections by pDNA encoding renilla luciferase in HuH-7 cells that stably expressed firefly luciferase. Both renilla (A) and firefly (B) luciferase expressions were evaluated simultaneously at defined time points. Arrows indicate the time of transfection set at every 24 h. Closed circles, squares and triangles represent expressions of P[Asp(DET)], P[Glu(DET)], and LPEI, respectively. Each data represents mean ± SEM (n = 6).

measurement of luciferase expressions after 24 and 48 h showed minimal differences among polymers of P[Asp(DET)], P[Glu(DET)], and LPEI at optimal N/P conditions (data not shown). To highlight the effects of the degradability of polymer on cells, we performed repeated transfections by administering polyplexes for every 24 h with refreshing of the culture medium. For this case, a polyplex solution formed at N/P = 5 with 0.25 μg pDNA was added to each well in a 96-well culture plate filled with 100 μL culture medium. Using these conditions, the final amine concentration corresponded to 0.04 mM in the medium, which would not have cytotoxic effects, even in the intact polymer form according to the results in Fig. 5.

As shown in Fig. 6A, P[Asp(DET)] resulted in a continuous increase in renilla expression until 72 h after repeated transfections for every 24 h using polyplex administration. Endogenous firefly luciferase expression remained constant during this time period (Fig. 6B). In contrast, using P[Glu(DET)], or LPEI, the renilla expression leveled off at 48 h after first transfection in parallel with the gradual down-regulation of endogenous firefly expression. Interestingly, the renilla expressions at 24 h post-transfection were comparable among polymers. Thus, these results suggest that, although a single dose of each polyplex caused minimal toxic effects on HuH-7 cells, repeated transfections resulted in cumulative toxicity when using the non-degradable polymers of P[Glu(DET)] and LPEI. By comparison, P[Asp(DET)] caused minimal cytotoxicity as P[Asp(DET)] was rapidly degraded to a non-toxic form.

HUVECs were also used for repeated transfections. Primary cells, such as HUVEC, are apt to be sensitive to the toxicity caused by cationic polymers. Indeed, as shown in Fig. 5B, the critical concentration of amines in the intact polymers that showed cytotoxicity to HUVEC was 0.01 mM, which was ¼ lower than for HuH-7 cells (0.04 mM). Thus, for these assays using HUVECs, a ¼ lower dose of polyplex prepared at N/P = 5 was applied. As shown in Fig. 7, P[Asp(DET)] showed a similar tendency with HuH-7 for a continuous increase in the luciferase expression during 72 h, whereas P[Glu(DET)] and LPEI showed decreases after 48 h of transfection.

For a detailed investigation focusing on cellular homeostasis, we analyzed the fluctuations in gene expressions of 31 frequently used housekeeping genes after transfections using P[Asp(DET)] or P[Glu(DET)]. These genes usually show uniform expressions,

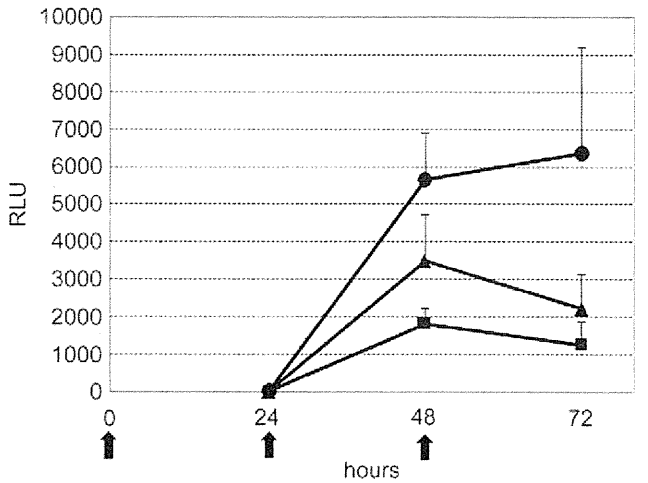

Fig. 7. Luciferase expression in HUVEC after repeated transfection. Arrows indicate the time of transfection set at every 24 h. Closed circles, squares and triangles represent expressions of P[Asp(DET)], P[Glu(DET)], and LPEI, respectively. Each data represents mean + SEM ($n = 6$).

although their expression profiles may vary in response to various external stimuli, such as cell stress [19]. Thus, variations in their expression profiles are good indicators for assessing cellular function, which reflect possible perturbations in cellular homeostasis. As shown in Fig. 8, all genes evaluated after transfection using P[Asp(DET)] remained within a 2-fold fluctuation compared to control cells. In contrast, P[Glu(DET)] induced larger fluctuations in the gene expressions, suggesting greater effects that altered the expressions of endogenous genes. Although the detailed mechanisms within cells should be investigated further, these results strongly suggest that P[Asp(DET)] maintained cellular homeostasis during the processes of transgene expression.

3.3. Cytokine induction after in vivo intraperitoneal injection

Finally, to evaluate the feasibility of P[Asp(DET)] biodegradability for clinical uses, we analyzed cytokine induction using *in vivo* experiments. Polymers were injected interperitoneally and serum concentrations of IL-6 and TNF-α were measured by ELISA after 4 h of injection. As shown in Fig. 9, the degradation products of P[Asp(DET)] induced these cytokines only to an extent comparable to normal saline, whereas the intact polymers induced detectable cytokine production. Considering the cationic nature of these polymers that could cause acute responses in the body, it may be difficult to completely eliminate cytokine induction after administration. However, these results indicate that once P[Asp(DET)] is degraded in the body it would cause almost no toxic reactions in a cumulative manner.

4. Discussion

In this study, we demonstrated that the biodegradability of P[Asp(DET)] contributed significantly to its safe and excellent transfection efficiency. *In vitro* evaluations of cytotoxicity due to the presence of polymers in the culture medium and by measurements of inflammatory cytokines after *in vivo* injection of polymers revealed that the degradation products of P[Asp(DET)] had almost no toxic effects on cells and tissues. Thus, P[Asp(DET)] has a clear advantage over other polymers as it can minimize the toxicity developed because of such polymers remaining within cells or in the body. Moreover, it is strongly suggested that the biodegradability of P[Asp(DET)] played an important role in maintaining cellular homeostasis after transgene expression in comparison with a non-degradable derivative polymer, P[Glu(DET)]. Because these two polymers possess identical amine units on their side chains, they showed similar properties of transgene expression and cytotoxicity just after the initial transfection (Day 1). However, on subsequent days, pharmacogenomic analysis showed remarkable differences in cell behavior, which ultimately affects long-term transgene expression. This type of cumulative toxicity observed

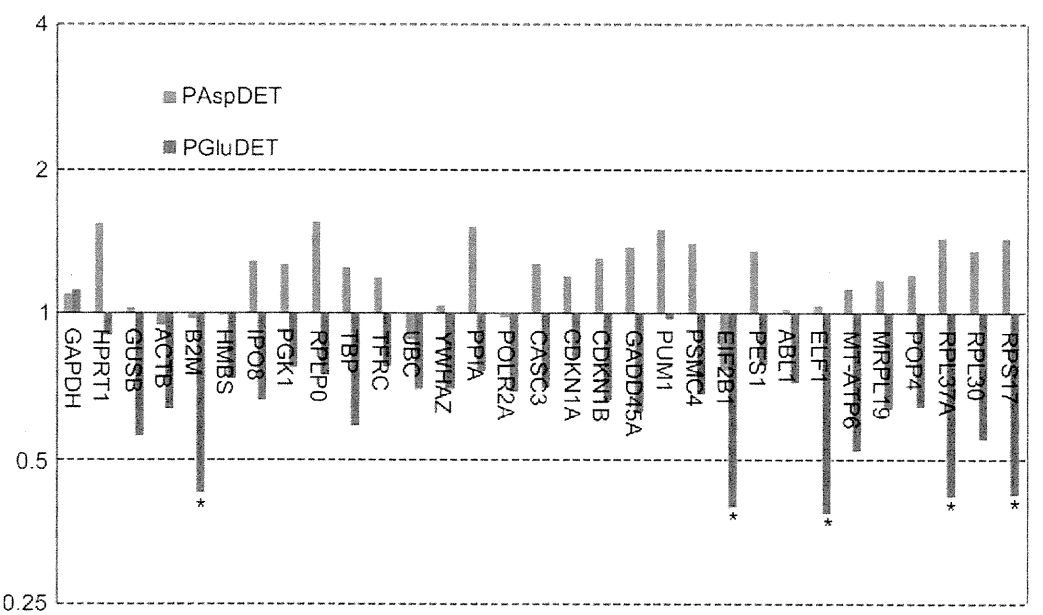

Fig. 8. Expression profiles of endogenous housekeeping genes in HUVEC after transfection using P[Asp(DET)] or P[Glu(DET)]. 31 genes were evaluated after 48 h of transfection using a Taqman express endogenous control plate. Asterisks indicate genes showing more than 2-fold fluctuation.

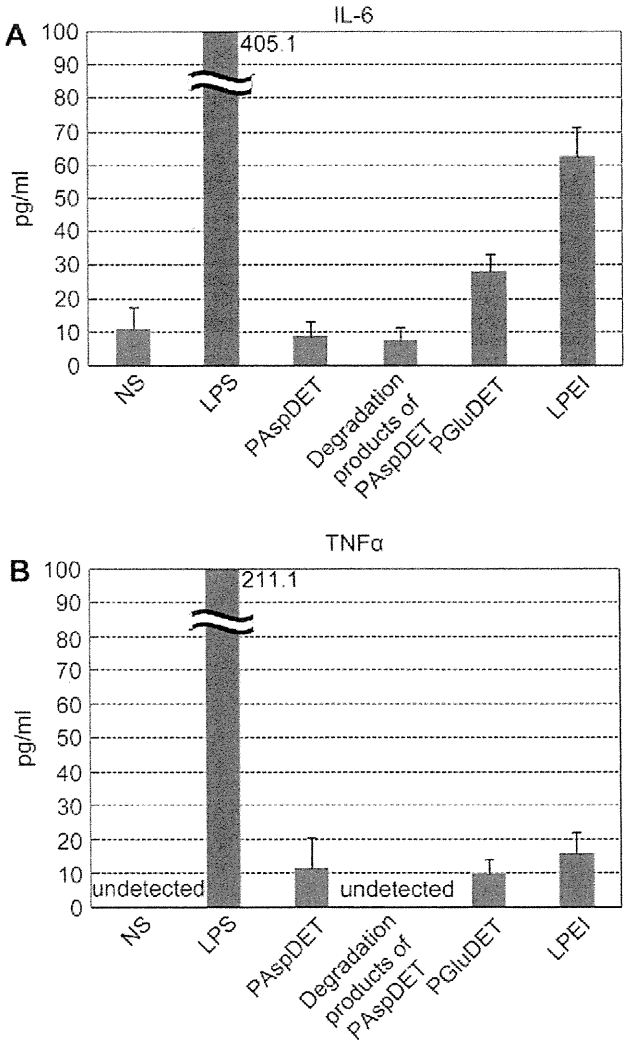

Fig. 9. Cytokine induction after intraperitoneal injection of polymers. Serum concentrations of IL-6 (A) and TNF-α (B) were measured after 4 h of injection of P[Asp(DET)], P[Glu(DET)], LPEI or the degradation products of P[Asp(DET)]. LPS was used as a positive control for measurements. Each data represents mean + SEM ($n = 4$).

with P[Glu(DET)] requires careful consideration when gene introduction is applied to regulate cell function and differentiation. For example, the production of induced pluripotent stem (iPS) cells by gene introductions of Oct3/4, Sox2, Klf4, and/or c-Myc using commercially available non-viral systems have been reported. However, unlike a retrovirus, repeated administrations on each day or at an interval of few days were required to obtain sufficient expressions of these factors in a sustained manner [20,21]. Because transgene expression obtained using non-viral carriers is primarily transient, repeated administrations of gene carriers are essential for applications like stem cell engineering. In this regard, the biodegradability of P[Asp(DET)] provides it with a clear advantage to be used clinically by minimizing cumulative toxicity caused by polymers remaining within cells or in the body.

It is interesting that P[Asp(DET)] and P[Glu(DET)] showed remarkable differences in their biodegradabilities due to the presence of an extra methylene group in the Glu backbone. As described briefly in the Results section, this phenomenon may be attributed to the entropically more favorable formation of a five-membered cyclic imide as compared with a six-membered cyclic imide. In natural peptides and proteins, succinimide formation by Asn mostly occurs via a nucleophilic attack of the amide nitrogen backbone on the side-chain carbonyl, followed by non-enzymatic deamidation. This results in occasional cleavage of the backbone, which has been estimated to be less than 10% of the deamidation [15]. Nevertheless, in this study, after one-month incubation of P[Asp(DET)] under physiological conditions, no fragments containing a deamidated Asp residue were identified by ESI-MS analysis (Fig. 3). After incubation for three months, final fragments corresponded to Asp(DET) monomer (Supplemental Fig. S3), indicating that selective cleavage of the backbone occurred in P[Asp(DET)] due to the increased nucleophilicity of the side-chain amide nitrogen. To be noted is that the degradation of P[Asp(DET)] was nearly restricted in a lower temperature (i.e., 4 °C) (Supplemental Fig. S4), which provides an advantage during purification, storage, and manipulation. The detailed mechanism of the backbone cleavage in N-substituted polyaspartamides is now under investigation and will be reported in the near future.

5. Conclusion

In this study, we demonstrated that facile degradability of P[Asp(DET)] to a non-toxic form under physiological conditions played an important role in its use as an effective gene carrier. Its degradation was induced by the cleavage of the PAsp backbone due to the self-catalytic reaction between the backbone and the side-chain amide nitrogen. In comparison with a non-degradable derivative polymer, P[Glu(DET)], P[Asp(DET)] achieved high and sustained transgene expression without affecting cellular homeostasis, which is of great importance as a practical system for non-viral gene introduction.

Acknowledgements

This work was financially supported in part by the Core Research Program for Evolutional Science and Technology (CREST) from Japan Science and Technology Corporation (JST) (K.K.), Grants-in-Aid for Scientific Research from the Japanese Ministry of Education, Culture, Sports, Science and Technology (K.I.), and Medical Research Grant on Traffic Accident from the General Insurance Association of Japan (K.I.). We appreciate Prof. Masaru Kato (The University of Tokyo) for kind help in the ESI-MS measurements. We also thank Ms. Satomi Ogura (The University of Tokyo) for technical assistance.

Appendix

Figures with essential colour discrimination. Certain figures in this article, in particular Figs. 2 and 8 may be difficult to interpret in black and white. The full colour images can be found in the on-line version, at doi:10.1016/j.biomaterials.2009.11.072.

Appendix. Supplementary information

Supplementary data associated with this article can be found, in the online version, at doi:10.1016/j.biomaterials.2009.11.072.

References

[1] De Smedt SC, Demeester J, Hennink WE. Cationic polymer based gene delivery systems. Pharm Res 2000;17:113–26.
[2] Schaffert D, Wagner E. Gene therapy progress and prospects: synthetic polymer-based systems. Gene Ther 2008;15:1131–8.
[3] Itaka K, Kataoka K. Recent development of nonviral gene delivery systems with virus-like structures and mechanisms. Eur J Pharm Biopharm 2009;71:475–83.

[4] Boussif O, Lezoualc'h F, Zanta MA, Mergny MD, Scherman D, Demeneix B, et al. A versatile vector for gene and oligonucleotide transfer into cells in culture and in vivo: polyethylenimine. Proc Natl Acad Sci U S A 1995;92:7297–301.
[5] Kanayama N, Fukushima S, Nishiyama N, Itaka K, Jang WD, Miyata K, et al. A PEG-based biocompatible block catiomer with high buffering capacity for the construction of polyplex micelles showing efficient gene transfer toward primary cells. Chem Med Chem 2006;1:439–44.
[6] Masago K, Itaka K, Nishiyama N, Chung UI, Kataoka K. Gene delivery with biocompatible cationic polymer: pharmacogenomic analysis on cell bioactivity. Biomaterials 2007;28:5169–75.
[7] Akagi D, Oba M, Koyama H, Nishiyama N, Fukushima S, Miyata T, et al. Biocompatible micellar nanovectors achieve efficient gene transfer to vascular lesions without cytotoxicity and thrombus formation. Gene Ther 2007;14:1029–38.
[8] Itaka K, Ohba S, Miyata K, Kawaguchi H, Nakamura K, Takato T, et al. Bone regeneration by regulated in vivo gene transfer using biocompatible polyplex nanomicelles. Mol Ther 2007;15:1655–62.
[9] Harada-Shiba M, Takamisawa I, Miyata K, Ishii T, Nishiyama N, Itaka K, et al. Intratracheal gene transfer of adrenomedullin using polyplex nanomicelles attenuates monocrotaline-induced pulmonary hypertension in rats. Mol Ther 2009;17:1180–6.
[10] Miyata K, Oba M, Nakanishi M, Fukushima S, Yamasaki Y, Koyama H, et al. Polyplexes from poly(aspartamide) bearing 1,2-diaminoethane side chains induce pH-selective, endosomal membrane destabilization with amplified transfection and negligible cytotoxicity. J Am Chem Soc 2008;130:16287–94.
[11] De Marre A, Soyez H, Schacht E, Pytela J. Improved method for the preparation of poly[N5-(2-hydroxyethyl)-L-glutamine] by aminolysis of poly(γ-benzyl-L-glutamate). Polymer 1994;35:2443–6.
[12] Neuse E, Perlwitz A, Schmitt S. Water-soluble polyamides as potential drug carrier. III. Relative main-chain stabilities of side chain-functionalized aspartamide polymers on aqueous-phase dialysis. Die Angewandte Makromolekulare Chemie 1991;192:35–50.
[13] Geiger T, Clarke S. Deamidation, isomerization, and racemization at asparaginyl and aspartyl residues in peptides. Succinimide-linked reactions that contribute to protein degradation. J Biol Chem 1987;262:785–94.
[14] Johnson BA, Shirokawa JM, Hancock WS, Spellman MW, Basa LJ, Aswad DW. Formation of isoaspartate at two distinct sites during in vitro aging of human growth hormone. J Biol Chem 1989;264:14262–71.
[15] Wright HT. Nonenzymatic deamidation of asparaginyl and glutaminyl residues in proteins. Crit Rev Biochem Mol Biol 1991;26:1–52.
[16] Tyler-Cross R, Schirch V. Effects of amino acid sequence, buffers, and ionic strength on the rate and mechanism of deamidation of asparagine residues in small peptides. J Biol Chem 1991;266:22549–56.
[17] Liu DT. Deamidation: a source of microheterogeneity in pharmaceutical proteins. Trends Biotechnol 1992;10:364–9.
[18] Bernard T, Joachim MM. The hydrolysis of peptides. In: Hydrolysis in drug and prodrug metabolism. Wiley-VCH; 2003. p. 236–358.
[19] Thellin O, Zorzi W, Lakaye B, De Borman B, Coumans B, Hennen G, et al. Housekeeping genes as internal standards: use and limits. J Biotechnol 1999;75:291–5.
[20] Okita K, Nakagawa M, Hyenjong H, Ichisaka T, Yamanaka S. Generation of mouse induced pluripotent stem cells without viral vectors. Science 2008;322:949–53.
[21] Gonzalez F, Barragan Monasterio M, Tiscornia G, Montserrat Pulido N, Vassena R, Batlle Morera L, et al. Generation of mouse-induced pluripotent stem cells by transient expression of a single nonviral polycistronic vector. Proc Natl Acad Sci U S A 2009;106:8918–22.